Measurement Report: Wintertime new particle formation in the rural area of North China Plain: influencing factors and possible formation mechanism

Juan Hong[1,2†*], Min Tang[1,2†], Qiaoqiao Wang[1,2*], Nan Ma[1,2], Shaowen Zhu[1,2], Shaobin Zhang[1,2], Xihao Pan[1,2], Linhong Xie[1,2], Guo Li[3], Uwe Kuhn[3], Chao Yan[4], Jiangchuan Tao[1,2], Ye Kuang[1,2], Yao He[1,2], Wanyun Xu[5], Runlong Cai[6], Yaqing Zhou[1,2], Zhibin Wang[7], Guangsheng Zhou[5], Bin Yuan[1], Yafang Cheng[3], Hang Su[3]

[1]Institute for Environmental and Climate Research, Jinan University, Guangzhou, Guangdong 511443, China

[2]Guangdong-Hongkong-Macau Joint Laboratory of Collaborative Innovation for Environmental Quality, Guangzhou, China

[3]Multiphase Chemistry Department, Max Planck Institute for Chemistry, Mainz 55128, Germany

[4]School of Atmospheric Sciences, Joint International Research Laboratory of Atmospheric and Earth System Sciences, Nanjing University, Nanjing, China

[5]Hebei Gucheng, Agrometeorology, National Observation and Research Station, Chinese Academy of Meteorological Sciences, Beijing, 100081, China

[6]Institute for Atmospheric and Earth System Research/Physics, Faculty of Science, University of Helsinki, Helsinki, FI00014, Finland

[7]College of Environmental and Resource Sciences, Zhejiang University, Zhejiang Provincial Key Laboratory of Organic Pollution Process and Control, Hangzhou 310058, China

[†]These authors contributed equally to this work.

[*]Correspondence: Qiaoqiao Wang (qwang@jnu.edu.cn) and Juan Hong (juanhong0108@jnu.edu.cn)

Abstract:

The high concentration of fine particles as well as gaseous pollutants makes polluted areas, such as the urban setting of North China Plain (NCP) of China, a different environment for NPF compared to many clean regions. Such conditions also hold for other polluted environments in this region, for instance, the rural area of NCP, yet the underlying mechanisms for NPF remain less understood owing to the limited observations of particles in the sub-3nm range. Comprehensive measurements, particularly covering the particle number size distribution down to 1.3 nm, were conducted at a rural background site of Gucheng (GC) in the North China Plain (NCP) from 12 November to 24 December in 2018. Five NPF events during the 39 effective days of measurements for the campaign were identified, with

删除[Tang Min]: 4

the mean particle nucleation rate ($J_{1.3}$) and growth rate ($GR_{1.3-2.4}$) were 22.0 $cm^{-3}·s^{-1}$ and 3.9 $nm·h^{-1}$, respectively. During these five days, NPF concurrently occurred at an urban site in Beijing. Sharing similar sources and transport paths of air masses arriving at our site to that of urban Beijing, we hypothesis that NPF events during these days in this region might be a regional phenomenon. The simultaneous occurrence of NPF in both places implies that H_2SO_4-amine nucleation, concluded for urban Beijing there, could probably be the dominating mechanism for NPF at our rural site. The higher concentration of sulfuric acid during many non-event days compared to that of event days indicates that the content of sulfuric acid may not necessarily lead to NPF events under current atmosphere. Only when the condensation sink or coagulation sink was significantly lowered, atmospheric NPF occurred, implying that CS or CoagS are the dominating factor controlling the occurrence of NPF for present rural environment of NCP, being quite similar to the feature at urban Beijing.

Keywords: new particle formation, particle number size distribution, condensational sink, nucleation mechanism.

删除[Tang Min]: 4

删除[Tang Min]: 4

删除[洪娟]: 9

删除[洪娟]: 1

删除[洪娟]: 0.5

删除[洪娟]: 4

设置格式[洪娟]: 字体: （默认）Calibri, 小四, 非倾斜

设置格式[洪娟]: 字体: （默认）Calibri, 小四, 非倾斜

设置格式[洪娟]: 字体: （默认）Calibri, 小四, 非倾斜

删除[洪娟]: During these five days, NPF concurrently occurred in an urban site in Beijing, indicating that NPF events during these days in this region might be a regional phenomenaphenomenon. The simultaneous occurrence of NPF in both placesThis implies that H2SO4-amine nucleation, concluded for urban Beijing there, could also be the dominating mechanism for NPF at our rural site.

设置格式[洪娟]: 字体: （默认）Calibri, 小四, 非倾斜

删除[洪娟]: The condensation sink or coagulation sink for the survival of newly-formed and small clusters are the dominating factor controlling the occurrence of NPF under current atmosphere, whereas the contribution from the available H2SO4 cannot be neglected, either. This

删除[洪娟]: is slightly different from that of

删除[洪娟]: , where CS mainly determines whether NPF takes place or not

1. Introduction

Atmospheric new particle formation (NPF) is a major source of the global particles in terms of number concentration and size distribution (Kulmala et al., 2004) and is considered to contribute up to half of the global cloud condensation nuclei (CCN) budget in the lower troposphere (Spracklen et al., 2006; Dunne et al., 2016). In general, NPF consists of two consecutive processes: a) the formation or nucleation of molecular clusters by low-volatile gaseous substances, and b) their subsequent growth to detectable sizes or even larger, at which these particles may act as CCN or contribute to the particle mass concentration (Kulmala et al., 2000; Zhang et al., 2012).

Numerous laboratory measurements and field studies have shown that sulfuric acid molecules (H_2SO_4) are one of the key precursors to form molecular clusters for nucleation (Nieminen et al., 2010; Sipilä et al., 2010; Kirkby et al., 2011; Riccobono et al., 2014; Stolzenburg et al., 2020). However, these H_2SO_4 clusters relevant to atmospheric nucleation are typically quite small, i.e., with diameters below 1.5 nm, at which the detection efficiency of traditional instruments specific for NPF was usually unsatisfactory (Kulmala et al., 2013). This had led to large uncertainties in the measured formation rate of newly formed particles and thus required precise measurements of these clusters or particles down to sub-3 nm. Upon recently, progress such as the use of a particle size magnifier (PSM) (Vanhanen et al., 2011; Xiao et al., 2015), a neutral cluster and air ion spectrometer (NAIS) (Mirme and Mirme, 2013) and a chemical ionization atmospheric pressure interface time of-flight mass spectrometer (CI-APi-TOF) (Jokinen et al., 2012) make it possible to directly measure the number concentration of clusters in the 1-3 nm size range. Benefit from these novel techniques, observations have found that the growth of H_2SO_4 clusters would be significantly promoted after stabilized by other precursors like amines, ammonia or iodine species (Berndt et al., 2010; Kirkby et al., 2011; Almeida et al., 2013; Riccobono et al., 2014; Kürten et al., 2016; Sipilä et al., 2010). Furthermore,

删除[Tang Min]: s
设置格式[洪娟]: 下标
设置格式[洪娟]: 下标
删除[洪娟]: are is
设置格式[Juan Hong]: 丹麦语
设置格式[Juan Hong]: 英语(美国)
设置格式[Juan Hong]: 下标, 英语(美国)
设置格式[Juan Hong]: 英语(美国)
设置格式[Juan Hong]: 下标, 英语(美国)
设置格式[Juan Hong]: 英语(美国)
设置格式[Juan Hong]: 英语(美国)
设置格式[Juan Hong]: 英语(美国)
设置格式[Juan Hong]: 英语(美国)
删除[洪娟]: -
删除[洪娟]: (Vanhanen et al., 2011;
设置格式[洪娟]: 非突出显示
设置格式[洪娟]: 非突出显示
删除[Tang Min]: (Pushpawela et al., 2019; Sulo et al., 2020)
设置格式[Juan Hong]: 英语(美国)
设置格式[Juan Hong]: 英语(美国)
设置格式[Juan Hong]: 英语(美国)
设置格式[Juan Hong]: 英语(美国)
设置格式[Juan Hong]: 英语(美国)
设置格式[Juan Hong]: 非突出显示, 英语(美国)
设置格式[洪娟]: 非突出显示
设置格式[Juan Hong]: 英语(美国)
设置格式[洪娟]: 非突出显示
删除[Tang Min]: (Kürten et al., 2016; Sulo et al., 2020)
设置格式[Tang Min]: 突出显示
设置格式[Juan Hong]: 突出显示, 英语(美国)
设置格式[Tang Min]: 突出显示
设置格式[Juan Hong]: 突出显示, 英语(美国)
设置格式[Tang Min]: 突出显示

oxidation products from volatile organic compounds, for instance, highly oxidized organic compounds, were suggested to be important contributors to atmospheric nucleation (Ehn et al., 2014; Bianchi et al., 2016; Kirkby et al., 2016; Tröstl et al., 2016).

The North China Plain (NCP) of China, has been suffering heavily from the highly complex air pollution since decades (Ma et al., 2016; Shen et al., 2018; Zhang et al., 2020), owing to the high emissions or formation of different pollutants such as SO_2, NH_3, VOCs as well as fine particles from various sources (Guo et al., 2014; Zhang et al., 2015). Due to the high concentration of pre-existing particles, previous studies considered that in the NCP, less NPF would occur as the newly-formed particles would be scavenged much faster before growing. By contrast, atmospheric NPF was still frequently observed in this region (Chu et al., 2019; Deng et al., 2020; Cai et al., 2021), being more often than theoretically predicted (Kulmala et al., 2014), indicating that the underlying mechanisms for NPF in this area might be different, that those mechanism previously found for other environments might not be completely applicable. The higher concentration of these gaseous precursors makes this region an unique condition for NPF compared to relatively clean environments (Kulmama et al., 2016; Yu et al., 2017; Wang et al., 2017), further supporting the hypothesis of different formation mechanisms and thereby distinct features of NPF events in this region. These doubts concerning NPF in the NCP, however, still remain to be elucidated due to limitations of comprehensive measurements, particularly for rural areas of the NCP, where observations regarding NPF was even more rare.

In addition, with respect to those existing studies concerning NPF in the NCP, they mainly focused on the measurements of particles beyond 3 nm. Without applicable instruments, observations of new particles down to sub-3nm was still quite limited (Fang et al., (2020); Zhou et al., (2020)), causing large uncertainties in the measured characteristics of NPF for current region. To fill the gap of measurements of particles or clusters in the size range of 1-3 nm and further advance our understanding of NPF in this region, particularly in the rural area of NCP, we conducted a comprehensive measurement campaign at a rural background site in

删除[洪娟]: participating in

删除[Tang Min]:

设置格式[Tang Min]: 突出显示, （复杂文种）

设置格式[洪娟 [2]]: 缩进: 首行缩进: 2 字符

删除[洪娟]: s

设置格式[洪娟]: 下标

设置格式[洪娟]: 下标

设置格式[Juan Hong]: 丹麦语

设置格式[Juan Hong]: 丹麦语

设置格式[Juan Hong]: 丹麦语

设置格式[Juan Hong]: 丹麦语

设置格式[Juan Hong]: 丹麦语

设置格式[Juan Hong]: 丹麦语

the NCP during 12 November to 24 December, 2018. By obtaining the particle number size distribution over a wide diameter range (1.3 nm - 10 μm), we aimed to investigate the characteristics of NPF events at the rural site in NCP during wintertime, find out which factors govern the occurring of NPF compared to other regions of NCP such as the urban areas and explore the potential mechanisms for NPF in this area.

删除[Tang Min]: 12

删除[Tang Min]: 24

删除[Tang Min]: 4

2. Experiment

2.1. Field measurements site

The measurements were conducted at Gucheng (GC) site (39°09'01.1"N 115°44'02.6"E), situated at an Ecological and Agricultural Meteorology Station (39°09' N, 115°44' E) of the Chinese Academy of Meteorological Sciences from 12 November to 24 December in 2018. The station is located in Dingxing county, Baoding city, Hebei Province, China, as seen in Fig.1 and surrounded by agricultural fields and sporadic villages. Being far from the urban and industrial emission areas, this site can be treated as a representative regional site in the northern part of NCP. More details about this site can be found in Lin et al. (2009) and Shen et al. (2018).

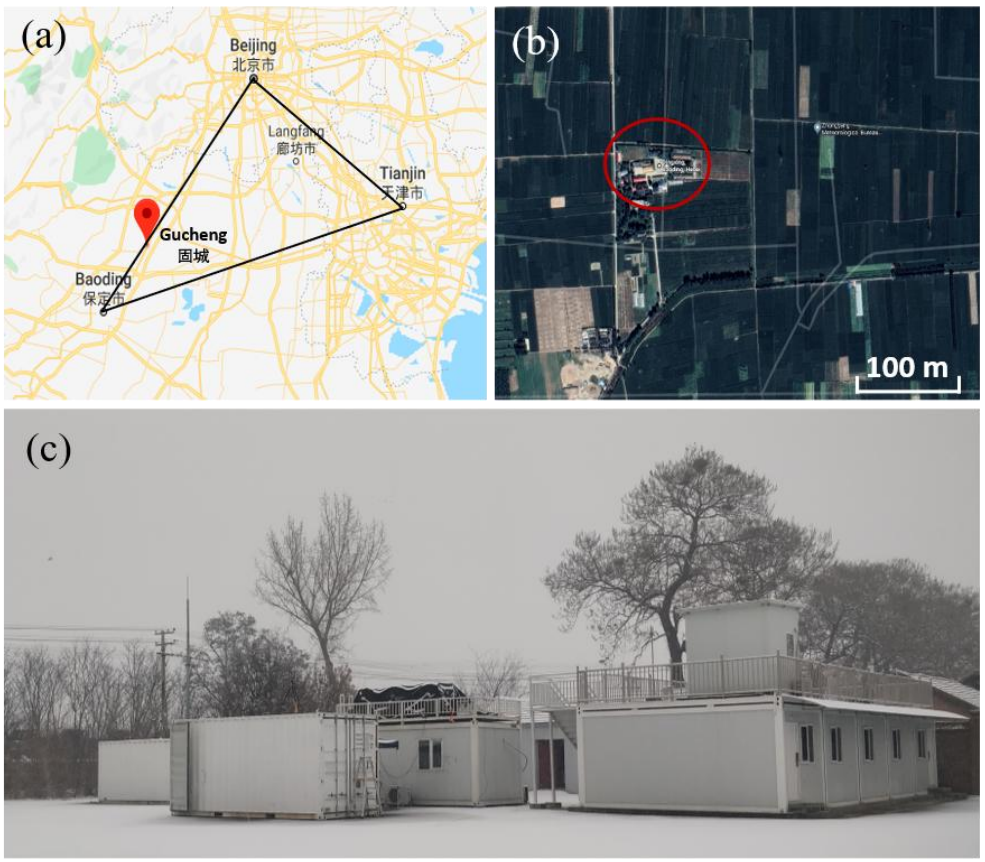

Figure 1. The upper panel shows the geographical location of the site (red dot and circled, © Google Maps), where our field measurements were carried out. The lower panel shows the measurement containers, where the sampling instruments were set up.

2.2. Measurements

2.2.1. Particle Number Size Distribution (PNSD) measurement

The aerosol sampling inlet was located on the rooftop of a measurement container, where room temperature was maintained at 22 ℃ (Fig1. c). The aerosol was sampled via a low-flow PM_{10} cyclone inlet, passed through a Nafion dryer, and directed to different instruments through stainless steel or conductive black tubings using an isokinetic flow splitter. The particle number size distribution of aerosol particles with diameters from 10 nm to 10000 nm was measured by using a scanning mobility particle sizer (SMPS, model TSI 3938) and an Aerodynamic Particle Size Spectrometer (APS, model TSI 3321) at a time resolution of around 5 minutes. The SMPS consisted of an electrostatic classifier (model TSI 3080) and a condensation particle counter (CPC, model TSI 3772).

设置格式[洪娟]: 下标

删除[洪娟]: , a differential mobility analyzer (DMA, model TSI 3081)

2.2.2. Sub-3nm Particle Number Concentration measurement

Sub-3nm particles were measured with an Airmodus nano Condensation Nucleus Counter system (nCNC, model A11), consisting of a Particle Size Magnifier (PSM, model A10) and a butanol condensation particle counter (CPC, model A20) (Vanhanen et al., 2011). The Airmodus PSM uses diethylene glycol as the working fluid to activate and grow nano-sized particles. Specifically, the PSM was operated under the scanning mode that the diethylene glycol flow was varied between 0.1 to 1.3 $L \cdot min^{-1}$. Thus, the number size distribution of five different size bins, i.e., 1.3-1.4, 1.4-1.6, 1.6-1.9, 1.9-2.4, and 2.4-3.7 nm was obtained. Owing to the data quality, only the former four size bins data were used in this study. During this campaign, the duration of each scan was completed within around 240 s.

删除[Tang Min]:

删除[Tang Min]: (Kangasluoma et al., 2016)

删除[Tang Min]: 4

删除[Tang Min]: 39

删除[Tang Min]: 39

删除[Tang Min]: 0

删除[洪娟]: 0

删除[Tang Min]: 4

删除[Tang Min]: 4

删除[Tang Min]: 0

删除[Tang Min]: 0

删除[Tang Min]: 0

2.2.3. Pollutant gases, PM2.5 and meteorological parameters measurement

Concentration of trace gases, including SO_2, O_3, CO and NOx, was measured continuously during this campaign using different Thermo Fisher Analysers (model

删除[Tang Min]: Themo Fisher Analyzers

43i-TLE, 49i, 48i, and 42i), respectively, at a time resolution of 1 minute. The concentration of oxygenated volatile organic compounds (OVOCs) was measured with an iodide-adduct long time-of-flight chemical ionization mass spectrometer (I-CIMS, Aerodyne, US) at a time resolution of 10-30 s for current study.

In addition, ambient meteorological conditions, such as wind speed, wind direction, temperature, relative humidity and solar radiation, were also regularly measured in another building, which is located about 20 meters to the southwest of the container, at the same observational site.

Furthermore, in order to investigate the influence of the origins and transport paths of air parcels to the local atmospheric compositions during NPF events, 72-h back trajectories of air masses arriving at 100 m above ground level at our GC site were analyzed using the HYbrid Single-Particle Lagrangian Integrated Trajectory (HYSPLIT) model for the classified event days.

设置格式[洪娟]: 字体: （默认）Calibri, 小四, 非倾斜

设置格式[洪娟]: 字体: （默认）Calibri, 小四, 非倾斜

删除[洪娟]: The non-refractory submicron aerosol chemical composition was measured by an Aerosol Chemical Speciation Monitor (ACSM, Aerodyne, USA) (Sun et al., 2012) and the black carbon mass concentration was measured by a 7-wavelength aethalometer (model AE-33, Magee Scientific Inc., USA) (Petzold et al., 2013) using a PM2.5 inlet.

设置格式[洪娟]: 字体: （默认）Calibri, 小四, 非倾斜

2.3. Data processing

2.3.1. Formation Rate (J_{Dp}) and Growth Rate (GR)

J_{Dp} defines the formation rate of atmospheric particles at a certain diameter (D_P) and can be calculated according to Kulmala et al. (2012) as:

$$J_{D_p} = \frac{dN_{\Delta D_p}}{dt} + CoagS_{\Delta D_p} \times N_{\Delta D_p} + \frac{1}{\Delta D_p} GR_{\Delta D_p} \times N_{\Delta D_p}$$

where N is the particle number concentration between the diameter dp_2 and dp_1 (denotes as ΔD_P), $CoagS$ is the coagulation sink of particles, GR is the particle growth rate out of the selected size bin.

In our study, we used two independent methods to calculate GR. One is the maximum concentration method (Kulmala et al., 2012), being mainly for the PSM data. The other is based on the variation in geometric mean diameters of particle number size distribution, which is derived by fitting the PNSD into 2 or 3 log-normal modes using an automatic algorithm (DO-FIT model) (Hussein et al., 2005), mainly for SMPS data.

$$GR = \frac{ddp}{dt} = \frac{\Delta dp}{\Delta t} = \frac{dp_2 - dp_1}{t_2 - t_1}$$

where dp_1 and dp_2 were particle diameters at time t_1 and t_2, respectively.

2.3.2. Condensation Sink (CS) and Coagulation Sink ($CoagS$)

CS describes how fast the low-volatility molecules condense onto pre-existing aerosols and can be expressed as (Kulmala et al., 2012):

$$CS = 2\pi D \int_0^{dpmax} \beta_{m,dp} dp N_{dp} ddp = 2\pi D \sum_{dp} \beta_{m,dp} dp N_{dp}$$

where *D* is the diffusion coefficient of the condensing vapor, which is usually referred to sulfuric acid and $\beta_{m,dp}$ is the mass flux transition correction factor.

$CoagS$ represents how fast the freshly formed particles are lost to pre-existing particles through coagulation and can be calculated as :

$$CoagS_{dp} = \int K(dp, dp') n(dp) ddp' \cong \sum_{dp'=dp}^{dp'=max} K(dp, dp') N_{dp'}$$

where, $K(dp, dp')$ is the collision efficiency between particles at the diameter from dp to dp'.

2.3.3. Sulfuric Acid proxy (*SA* proxy)

SA was considered as one of the key precursors responsible for particle nucleation in the atmosphere. However, no direct measurement for the concentration of SA was available in current study. We therefore used a proxy variable to substitute the concentration of SA, as SA is mainly produced by the oxidation of SO_2 by OH radicals, which can be approximated by the UV-B intensity (Petäjä et al., 2009). Thus, the proxy concentration of SA can be calculated by Lu et al. (2019):

$$SA\ proxy = 0.0013 \cdot UVB^{0.13} \cdot [SO_2]^{0.40} \cdot CS^{-0.17} \cdot ([O_3]^{0.44} + [NO_x]^{0.41})$$

设置格式[洪娟]: 缩进: 首行缩进: 8.5 毫米

设置格式[洪娟]: 下标

删除[Tang Min]:

删除[Tang Min]: (

删除[Tang Min]: ,

删除[Tang Min]: (Zhu et al., 2017)

删除[洪娟]: <math>

where, <math> is a scaling constant and was assumed to be 2.3×10^{-9} $m^2/(W$<math>.

2.3.4. Classification of NPF event

Days of NPF events was classified according to the method proposed by Dal Maso et al. (2005) and Kulmala et al. (2012), in which (a) a burst in the concentration of sub-3 nm particles or clusters was observed and (b) these particles had a continuous growth over a time span of hours (e.g., usually more than ten hours). If no clear growth of these newly formed particles (sub-3 nm particles) can be identified, the day was classified as an undefined day. The day without both the burst of sub-3 nm particles and their subsequent growth was considered as a non-event day.

2.3.5. Indicator for the occurrence of NPF

Previously, McMurry et al. (2005)proposed a dimensionless criterion, *L*, to predict the occurrence of NPF events in the atmosphere. After being validated in diverse atmospheric environments (Kuang et al., 2010; Cai et al., 2017), *L* has been used to investigate the governing factors for NPF events under typical atmospheric conditions. Upon recently, Cai et al. (2021a) proposed a new indicator, *I*, on the basis of *L*, which only considered H_2SO_4 to drive the growth. The new indicator was calculated by further taking into account the condensation of other species, for instance, amines and has been suggested to be a good quantitative representation for the occurrence of NPF after comparing with *L* for NPF events observed at urban Beijing (Deng et al., 2020). The detailed information to calculated *I* can be found in (Cai et al., 2021a).

设置格式[洪娟]: 字体: （默认）Calibri, 小四, 非倾斜
删除[Tang Min]: (
删除[Tang Min]: ,
删除[Tang Min]: Dal Maso et al. (2005)
设置格式[洪娟]: 字体: （默认）Calibri, 小四, 非倾斜
删除[Tang Min]: Kulmala et al. (2012)
设置格式[洪娟]: 字体: （默认）Calibri, 小四, 非倾斜
删除[洪娟]: Days of NPF events was classified according t...
设置格式[Juan Hong]: 英语(美国)
设置格式[Juan Hong]: 英语(美国)
设置格式[Juan Hong]: 英语(美国)
设置格式[Juan Hong]: 英语(美国)
设置格式[Juan Hong]: 英语(美国)
设置格式[Juan Hong]: 英语(美国)
设置格式[洪娟 [2]]: 字体: 非倾斜, 字体颜色: 背景 2,...
设置格式[洪娟]: 2 级标题, 编号 + 级别: 3 + 编号样式...
设置格式[洪娟]: 项目符号和编号
设置格式[洪娟]: 字距调整: 0 磅
设置格式[洪娟]: 字体: （默认）Calibri, 小四, 非倾斜
删除[Tang Min]: McMurry et al. (2005)
删除[Tang Min]: (
删除[Tang Min]: ,
设置格式[洪娟]: 字体: （默认）Calibri, 小四, 非倾斜
删除[Juan Hong]: (
删除[Juan Hong]: Kuang et al., 2005;
设置格式[洪娟]: 字体: （默认）Calibri, 小四, 非倾斜
删除[Tang Min]: Cai et al., 2017;
删除[Juan Hong]: (Cai et al., 2017))
设置格式[洪娟]: 字体: （默认）Calibri, 小四, 非倾斜
删除[Juan Hong]: (
删除[Juan Hong]: ,
删除[Juan Hong]: Cai et al. (2021)
设置格式[洪娟]: 字体: （默认）Calibri, 小四, 非倾斜
删除[Tang Min]: (Deng et al., 2020)

3. Results and discussion

3.1. General characteristics of NPF at GC site

Figure 2 shows the time series of meteorological parameters (a: wind speed and direction, b: temperature and relative humidity) and aerosol properties (c: total surface and volume concentration, d and e: PNSD in the size range of 10 to 800 nm and particle number concentration in the range of 1.3 to 2.4 nm) during this field campaign. During our study, wind speed was typically quite low with an average of 1.18 $m \cdot s^{-1}$, indicating stagnant meteorological conditions for the limited dilution of air pollutants at the current site. The temperature and relative humidity (RH) show opposite diurnal variation over the observational period, with the highest temperature and lowest RH during daytime and vice versa during nighttime. The observed time series of concentration of different trace gases during current study is shown in Fig. S1. To be specific, the campaign-averaged concentration of CO, O_3, NO_X and SO_2 was 1394 ppb, 7 ppb, 83 ppb and 10 ppb, respectively.

According to the PNSD and PSM data, five days, with four of which having significant burst of sub-3 nm clusters as shown in Fig.2e, were classified as NPF events out of the total experimental period. It has to be noted that on the day of November 18, though PSM data was not available due to technical issues, clear growth of nucleation mode particles with a typical banana-shape PNSD was observed, lasting for more than 12 hours. These particles under the growth of such a long time should not be from traffic emissions or transported. Therefore, it was also classified as an event day in our study. Considering all these five NPF event, this corresponds to an NPF frequency of 12.8%, which was lower than those at an urban site (i.e., Beijing) in the same region during the same season Shen et al. (2018) (25.8%); Deng et al. (2020) (51.4%)). Similar findings were also observed in Yue et al. (2009) and Wang et al. (2013), that NPF frequencies were higher at the Beijing urban site than at the corresponding regional background or rural site. Yue et al. (2009) and Wang et al.

删除[洪娟]: s

设置格式[洪娟 [2]]: 缩进: 首行缩进: 2 字符

删除[Tang Min]: 4

删除[洪娟]: 0

设置格式[洪娟]: 字体: （默认）Calibri, 小四, 非倾斜

删除[洪娟]:

删除[洪娟 [2]]:

删除[洪娟]: According to the PNSD and PSM data, five da

设置格式[洪娟 [2]]: 缩进: 首行缩进: 2 字符, 行距: 1.

设置格式[洪娟]: 字体: （默认）Calibri, 小四, 非倾斜

设置格式[洪娟]: 字体: （默认）Calibri, 小四, 非倾斜

删除[Tang Min]: (

删除[Tang Min]: (

删除[Tang Min]: ,

删除[Tang Min]: Sun, Zhang,

删除[Tang Min]: ,

删除[Tang Min]: Shen et al. (2018)

设置格式[洪娟]: 字体: （默认）Calibri, 小四, 非倾斜

删除[Tang Min]: (

删除[Tang Min]: ,

删除[Tang Min]: Deng et al. (2020)

设置格式[洪娟]: 字体: （默认）Calibri, 小四, 非倾斜

删除[Tang Min]: (

删除[Tang Min]: ,

删除[Tang Min]: Yue et al. (2009)

设置格式[洪娟]: 字体: （默认）Calibri, 小四, 非倾斜

删除[Tang Min]: (Z. B.

删除[Tang Min]: ,

删除[Tang Min]: Wang et al. (2013)

设置格式[洪娟]: 字体: （默认）Calibri, 小四, 非倾斜

(2013) attributed this to the higher pollution level and correspondingly higher precursor content in the urban cities, leading to stronger NPF events there.

During our study, six days, with a slightly weak burst of sub-3 nm particles, were identified as undefined days as their formation and growth rate cannot be calculated accurately. For non-event days, we observed that during many of them some nucleation-mode particles with size above 10 nm did appear. However, we did not observe the burst of sub-3 nm clusters from the PSM measurements and moreover no clear growth of these particles can be identified. This indicates that these small particles probably are not from nucleation of H_2SO_4 with other species and their subsequent growth, but more likely local emissions (traffic exhausts) or long-range transported.

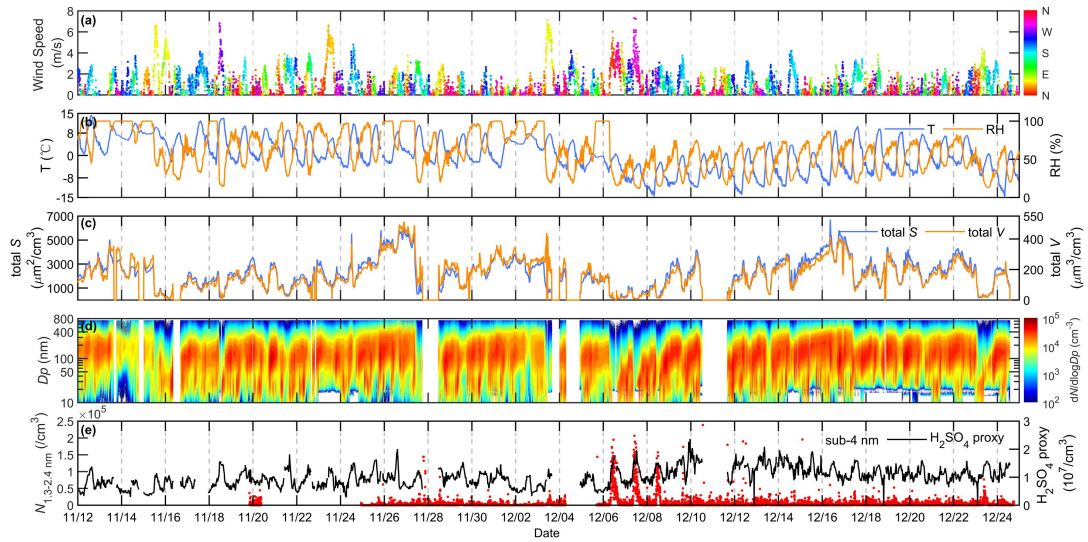

Figure 2. Time series of (a) wind speed and wind direction, (b) temperature, (*T*) and relative humidity (RH), (c) total particle surface and volume concentration calculated by using PNSD data, (d) measured PNSD in the size range of 10 - 800 nm, (e) particle number concentration in the range of 1.3 to 2.4 nm and H_2SO_4 proxy concentration during the entire measurement period (2018.11.12-2018.12.24). White portion indicates no data was available due to instrument maintenance or power failure. Note that white portion in the PNSD in the size range of 10 - 15 nm, indicating no available data, is due to the technical problems of our SMPS system; therefore data for that time period from a parallel SMPS covering sizes of 15 - 800 nm was used instead.

Figure 3 shows a typical NPF event on December 7 as an example. Northwest wind prevailed with elevated wind speed starting from around 8:00 o'clock, which was conducive to the diffusion of local pollutants, leading to a rapid decrease in CS

删除[Tang Min]: Yue et al. (2009) and Wang et al. (2013)

设置格式[洪娟]: 字体: （默认）Calibri, 小四, 非倾斜

删除[洪娟 [2]]:

设置格式[洪娟]: 字体: （默认）Calibri, 小四, 非突出显示

设置格式[洪娟]: 字体: （默认）Calibri, 小四, 非倾斜

设置格式[洪娟 [2]]: 缩进: 首行缩进: 2 字符

删除[洪娟]:

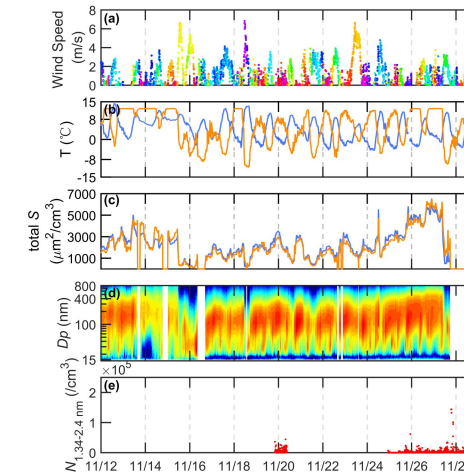

删除[Tang Min]:

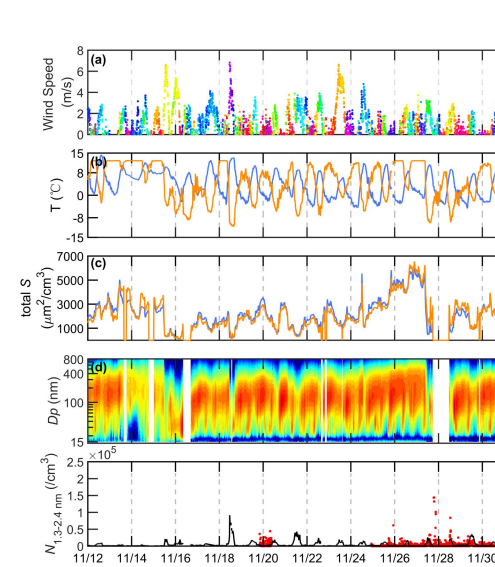

删除[洪娟]:

设置格式[洪娟]: 字体: （默认）Calibri

设置格式[洪娟]: 字体: （默认）Calibri

删除[洪娟]: Time series of (a) wind speed and wind direc

设置格式[Tang Min]: 突出显示

设置格式[Tang Min]: 突出显示

设置格式[洪娟 [2]]: 缩进: 首行缩进: 2 字符

删除[Tang Min]: dramatic

concurrently. At the same time, an obvious rise in H_2SO_4 concentration was observed, coinciding with a strong burst in the concentration of sub-3 nm clusters. Then, new particles with diameter larger than 10 nm, as shown in Fig. 3b, gradually formed by growth, exhibited as a visible banana shape in PNSD.

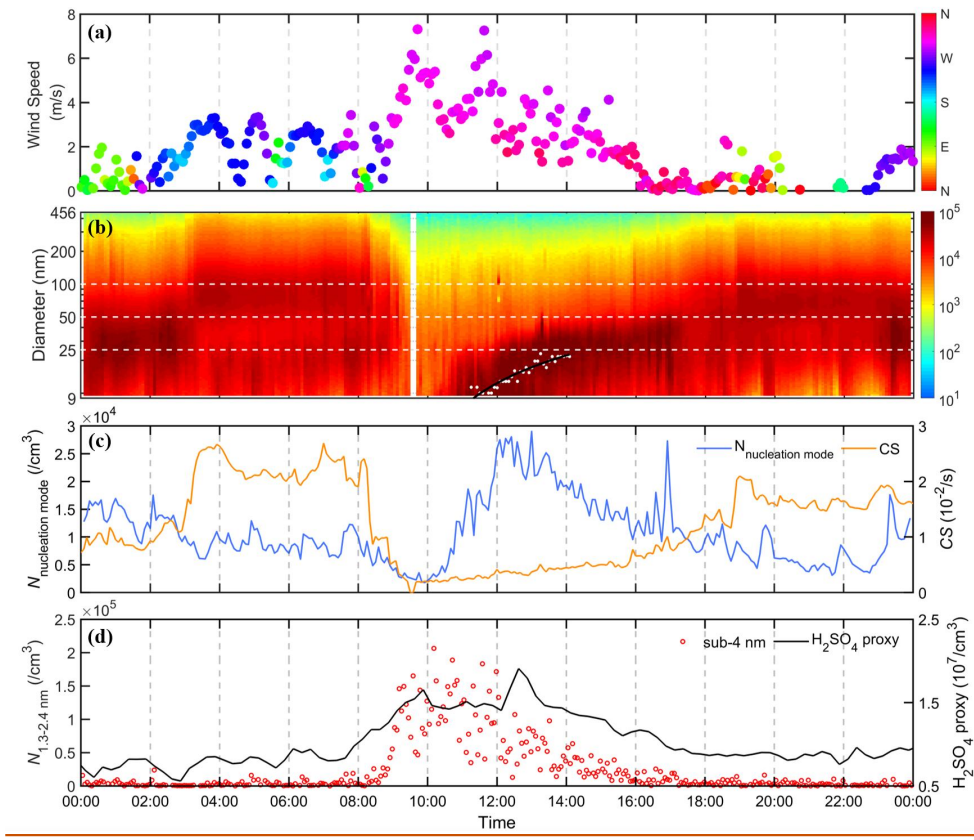

Figure 3. A case of NPF event on December 7 during this field campaign. Time series of (a) wind speed and wind directions, (b) the PNSD in the size range of 10 - 450 nm (The white dotted line represents the size with diameter at 25, 50, and 100 nm; black line represents the polynomial fit of the measured PNSD, (c) the particle number concentration of nucleation mode (9 - 25nm) and *CS*, (d) the number concentration of sub-3nm clusters and predicted concentration of sulfuric acid.

For all the identified NPF events, the formation rate of 1.3 nm ($J_{1.3}$) particles ranged from 6.0 $cm^{-3}·s^{-1}$ to about 30.4 $cm^{-3}·s^{-1}$ with an average value of 22.0 $cm^{-3}·s^{-1}$ at our GC site during the measurement period. Note that most atmospheric formation rates reported in China were based on the measured formation rates at relatively larger size, i.e., 3-10 nm, which are so called the "apparent" particle formation rates. In order to derive the formation rates of critical clusters from the "apparent" particle formation rates(Kulmala et al., 2017), the nuclei GR or GR at

设置格式[洪娟]: 下标

设置格式[洪娟]: 下标

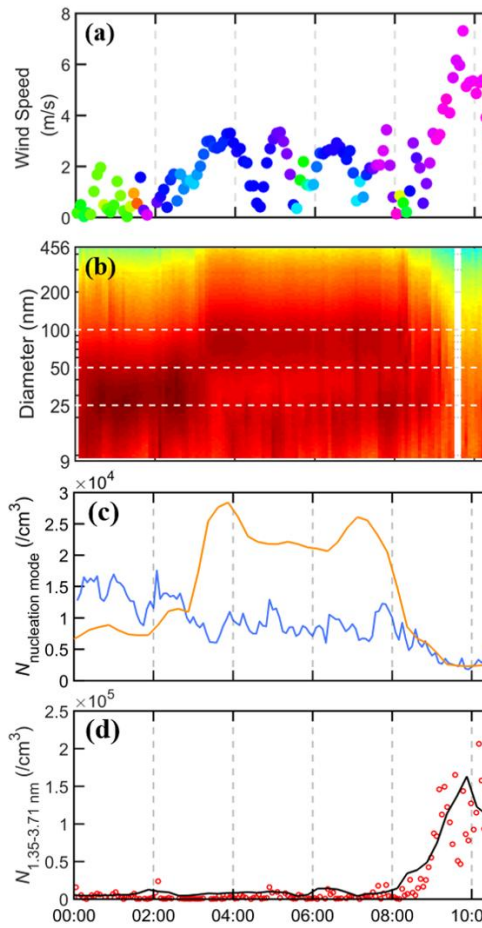

删除[洪娟]:

删除[洪娟]: 9

删除[洪娟]: 0

设置格式[洪娟 [2]]: 缩进: 首行缩进: 2 字符

删除[Tang Min]: 4

删除[Tang Min]: 4

删除[洪娟]: 8

删除[洪娟]: 1

删除[洪娟]: 4

删除[洪娟]: 8

删除[洪娟]: 9

删除[洪娟]: 1

设置格式[洪娟]: 字体: （默认）Calibri, 小四, 非倾斜

删除[Juan Hong]:

删除[Juan Hong]: (Kulmala et al., 2017)

设置格式[洪娟]: 字体: （默认）Calibri, 小四, 非倾斜

sub-3 nm is needed but usually remains unclear. Therefore, we focused more on the formation rate of particles at sizes below 3 nm in the following discussion. In principle, particle formation rate is inversely proportional to the CS, as the nucleation precursors or clusters would be scavenged more rapidly under higher CS conditions, leading to a slower nanoparticle formation with a lower *J*. However, as shown in Table 1, in spite of the higher CS, the particle formation rates at our site appear to be higher than those in clean environments. This kind of intensive NPF becomes more noticeable for those Chinese megacities, such as Shanghai, Beijing and Nanjing, having an even higher *J* and CS compared to that at our GC site. The most plausible explanation could be the higher abundance of nucleating precursors for NPF in those polluted atmospheres, which is indicated by the SA concentration, either measured in urban Shanghai and Nanjing or calculated in our study. To be specific, the mean SA proxy concentration during NPF at our GC site was around $1.4 \cdot 10^{7}$ cm^{-3}, a factor of around 30 higher than that at Hyytiälä in Finland (Nieminen et al., 2014). The SA concentration during NPF at Shanghai (Xiao et al., 2015) and Nanjing (Herrmann et al., 2014) was even higher, being around $4 \cdot 10^{7}$ cm^{-3}.

删除[洪娟]: It has to be noted that most atmospheric formation rates reported in China was were based on the measured formation rate at relatively larger size, i.e., 3-10 nm. However, according to Chu et al. (2019), large errors may associate with the deviations of *J* when using data at larger sizes as GR at sub-3 nm is needed but were typically unclear.

设置格式[洪娟]: 突出显示

删除[洪娟]: s

设置格式[洪娟]: 字体: （默认）Calibri, 小四, 非倾斜

设置格式[洪娟]: 字体: （默认）Calibri, 小四, 非倾斜

删除[洪娟]: The most plausible explanation could be the more higher abundance of nucleating precursors for NPF in those polluted atmosphere, which is indicatedclearly proved by the SA concentration, either measured or calculated.

删除[洪娟]: 7

删除[洪娟]: 6

删除[洪娟]: bove

删除[洪娟]: 10-20

删除[Tang Min]:

删除[Tang Min]:

删除[Tang Min]:

Table 1. Summaries of the parameters (average value) relevant for NPF event during wintertime in China and other countries.

Station	Period	Frequency	*J* ($cm^{-3}·s^{-1}$)	*GR* ($nm·h^{-1}$)	*CS* ($10^{-2}·s^{-1}$)	*SA* ($10^{6}·cm$
GC [R]	2018.11.18	-	3.15 (J_{10})	4.3	4.7	12.5
GC [R]	2018.12.06	-	29.7 ($J_{1.3}$)	1.8	0.7	14.4
GC [R]	2018.12.07	-	30.4 ($J_{1.3}$)	4.1	0.8	14.7
GC [R]	2018.12.08	-	21.8 ($J_{1.3}$)	8.1	2.7	13.5
GC [R]	2018.12.23	-	6.0 ($J_{1.3}$)	1.2	1.6	14.3
GC [R] (mean)	2018.11.12-12.24	12.8%	22.0 ($J_{1.3}$)	3.9	2.1	13.9
Thissio [UB]	2015.8-2016.8, 2017.2-2018.2[a]	10.3%	1.55 (J_{10})	3.48	0.79	6.33
New Delhi [U]	2002.10.26-2002.11.9	53.3%	7.3 (J_3)	14.9	5.75	-
Panyu [U]	Winter of 2011	21.3%	0.89 (J_{10})	5.1	5.5	-
Shanghai [U]	2013.11.25-2014.1.25	21%	188 ($J_{1.34}$)	11.4	6.0	37
Nanjing [U]	2011.11.18-2012.3.31	20%	33.2 (J_2)	8.5	2.4	45.3
Hongkong [U]	2010.10.25-2010.11.29	34.3%	2.94($J_{5.5}$)	3.86	0.8-6.2	9.17
Beijing [U]	2018.1.23-2018.3.31	51.5%	38 ($J_{1.5}$)	5.5	3.7	4.13
Ziyang [R]	2012.12.5-2013.1.5	23%	5.2(J_3)	3.6	7.4	6.7
Melpitz [R]	Winter of 2003-2006	3%	0.7 (J_3)	5.6	1.2	0.123
Melpitz [R]	Winter of 1996-1997	10%	4.9(J_3)	4.1	0.9	0.259
Pingyuan [R]	2017.11.3-2018.1.20	39.2%	164.2 ($J_{1.5}$)	3.9	1.9	2.45
Xinken [R]	2004.10.3-2004.11.5	25.9%	0.5-5.4(J_3)	2.2.-19.8	-	-
Solapur [R]	2018.10-2019.2	28.9%	0.22-10.07(J_{15})	1.2-13.8	0.6-3	-
Cyprus [RB]	2018.1-2018.2	69%	16.4($J_{1.5}$)	9.97	1.2	-
SEAS [O]	Winter of 2018	5%	2.95(J_{10})	14.35	4.5	-
SMEAR II [B]	Winter of 1996-2003	24.2%	0.2-1.1(J_3)	0.29-3.7	0.05-0.35	0.53

SEAS: the southeastern Arabian Sea

R: rural site UB: urban background site RB: rural background site U: urban site. B: background site O: ocean site

a: only in wintertime

-: no number

带格式表格[Tang Min]
删除[洪娟]: 27
删除[洪娟]: 4.
删除[洪娟]: 1
删除[洪娟]: 3
删除[洪娟]: 4
删除[Tang Min]: 4
删除[洪娟]: 4
删除[洪娟]: 4
删除[洪娟]: 0
删除[洪娟]: 4
删除[洪娟]: 8
删除[Tang Min]: 4
删除[洪娟]: 05
删除[洪娟]: 1
删除[洪娟]: 3
删除[洪娟]: 8
删除[洪娟]: 2
删除[Tang Min]: 4
删除[洪娟]: 1
删除[洪娟]: 4
删除[洪娟]: 9
删除[洪娟]: 8
删除[洪娟]: 1
删除[Tang Min]: 4
删除[洪娟]: 3
删除[洪娟]: 5
删除[洪娟]: 5
删除[洪娟]: 9
删除[洪娟]: 1
删除[Tang Min]: 4
删除[洪娟]: 7
删除[洪娟]: 15
删除[Tang Min]: H.

Although the formation rate of 1.3 nm particles is relatively high, the newly-formed particles at our GC site usually cannot grow into very large particles within a short time, indicative by their low GR. The average value of $GR_{1.3-2.4}$ and GR_{9-15} at our site was 0.5 nm·h^{-1} and 3.9 nm·h^{-1}, respectively, being generally lower than many clean environments (GR_{1-3} of 0.9 nm·h^{-1} for Hyytiälä (Kulmala, 2013), of 5.1 nm·h^{-1} for Jungfraujoch (Boulon et al., 2010)), but similar to those at urban Beijing (Chu et al., 2021) and rural Pingyuan (Fang et al., 2020). This could be attributed by the high CS or CoagS at those polluted environments as the growth of small particles is limited, which are more vulnerable to the coagulation scavenging. However, despite the high CoagS, the observed GR at Shanghai and Nanjing was still exceptionally high. This discrepancy suggests that besides the high concentration of precursors, mainly H_2SO_4, in polluted environments including both rural and urban sites, other precursors with different efficiency for nanoparticle growth, and other involving mechanisms, for instance, multiphase reactions, may all contribute to the nanoparticle growth, yet to be elucidated.

3.2. Potential mechanisms for NPF events in the rural NCP

To further understand the dominating nucleation mechanism in the rural atmosphere of NCP in China, we plotted the measured formation rate of 1.3 nm particles ($J_{1.3}$) against the simulated H_2SO_4 concentration and compared the results to previous studies conducted in different environments, as shown in Fig. 4. As illustrated by the significant correlation between the concentration of sulfuric acid and the particle formation rates, sulfuric acid is considered to be the driving species in the initial steps of NPF as confirmed conventionally. However, the obtained $J_{1.3}$-H_2SO_4 relationship for current environment appeared to deviate largely from those obtained by other studies. If only referring to the slope of the $J_{1.3}$-H_2SO_4 relationship, our results seem to approximate most to the ones measured by these CLOUD (The Cosmics Leaving OUtdoor Droplets chamber) experiments based on the mechanism of H_2SO_4-DMA nucleation. However, without the direct measurements of

设置格式[洪娟 [2]]: 缩进: 首行缩进: 2 字符
删除[Tang Min]: 4
删除[Tang Min]: 4
删除[洪娟]: 4
删除[洪娟]: /h
删除[洪娟]: /h
删除[洪娟]: /h
设置格式[洪娟]: 非突出显示
设置格式[洪娟]: 非突出显示
删除[洪娟]: /h
设置格式[洪娟]: 非突出显示
设置格式[洪娟]: 非突出显示
设置格式[洪娟]: 非突出显示
设置格式[洪娟]: 非突出显示
设置格式[洪娟]: 字体: （默认）Calibri, 小四, 非倾斜
删除[洪娟]: This could be attributed by the high CS or CoagS at those sites that small particles are vulnerable to the coagulation scavenging.
设置格式[洪娟]: 字体: （默认）Calibri, 小四, 非倾斜
设置格式[洪娟 [2]]: 缩进: 首行缩进: 2 字符

other potential precursors, the molecules stabilizing H_2SO_4 clustering still remain unclear.

Comparing the particle formation rates reported in different environments in China, our results were of the similar magnitude as that in Beijing (Cai et al., 2021b), an urban site in the NCP. It has to be noted that their study was conducted during a much longer time and completely covered the measurement period of our study. More importantly, during the five days of events in our study, NPF concurrently occurred at their measurement site (Liu et al., 2020). Additionally, for these five event days air masses arriving at our site followed similar transport paths to that at urban Beijing (see Fig. S2 as an example in the supplement), both originating from Siberia areas, where concentration of gaseous pollutants and particulate matter was typically quite low, through the northwest of the observational sites. Taking both evidence, we hypothesis that NPF events during these days in this area might be a regional phenomenon, sharing the same or similar nucleation mechanism. Cai et al. (2021) and Yan et al. (2021) further concluded that H_2SO_4-DMA was the dominating nucleation mechanism for urban Beijing with an additional support from the measured C2-amine concentration. Considering the similarities between these two sites, we speculated that the clustering of H_2SO_4 with DMA may also dominate the nucleation process at our site during winter, though future work is needed to verify current hypothesis.

On the other hand, we noticed that our results deviate significantly from the measured formation rate at Pingyuan (Fang et al., 2020), another rural site in the NCP. They concluded that neither H_2SO_4-NH_3 nor H_2SO_4-DMA mechanisms could fully explain their observed particle formation rate but suggested that gaseous dicarboxylic acids were the dominating species for the initial step of H_2SO_4 clustering under diacid-rich environment. Being likewise the rural environment of NCP, we cannot completely rule out the contribution of dicarboxylic acids to the H_2SO_4 stabilizing. However, as illustrated in Fig. S4, the concentration of these four dicarboxylic acids during NPF events were in general lower than that during non-event days. Furthermore, during the daytime of events days when NPF was

删除[洪娟]: To further understand the dominating nucleation mechanism in the rural atmosphere of NCP in China, we plotted the measured formation rate of 1.34 nm particles ($J_{1.34}$) against the simulated H_2SO_4 concentration and compared the results to previous studies conducted in

删除[洪娟 [2]]:

设置格式[洪娟]: 字体: （默认）Calibri, 小四, 非倾斜

设置格式[洪娟]: 字体: （默认）Calibri, 小四, 非倾斜

设置格式[洪娟]: 字体: （默认）Calibri, 小四, 非倾斜

设置格式[洪娟]: 字体: （默认）Calibri, 小四, 非倾斜

设置格式[洪娟]: 字体: （默认）Calibri, 小四, 非倾斜

设置格式[洪娟]: 字体: （默认）Calibri, 小四, 非倾斜

设置格式[洪娟]: 字体: （默认）Calibri, 小四, 非倾斜

删除[洪娟]: For NPF in China, the $J_{1.34}$-H_2SO_4 relationship in our results were also close to that in Beijing (Cai et al., 2021), an urban site in the NCP, but with a lower formation rate under similar H2SO4 level. Cai et al. (2021) and Yan et al. (2021) concluded that H2SO4-DMA was the dominating

设置格式[Tang Min]: 突出显示

删除[洪娟 [2]]:

删除[Tang Min]: s

设置格式[洪娟]: 下标

设置格式[洪娟]: 下标

设置格式[洪娟]: 下标

设置格式[洪娟]: 下标

设置格式[洪娟]: 下标

设置格式[洪娟]: 下标

设置格式[洪娟]: 下标

设置格式[洪娟]: 下标

设置格式[洪娟]: 下标

设置格式[洪娟]: 字体: （默认）Calibri, 小四, 非倾斜

typically initiated, the signals of these diacids obtained from the I-CIMS did not show clear increase, unlike sulfuric acid, but rather elevated during the night time (see Fig. S5), being obviously different from the case of Pingyuan. Hence, the involvements of diacids during the initial steps of nucleation under current rural atmosphere might not hold. This statement does not necessarily mean that our previous inference was incorrect, but on the other hand, provides some hints that though NPF events in the NCP is regional, there might be no uniform theory but multiple mechanisms coexisting to explain its feature with the dominating one varying upon different emission patterns or meteorological conditions.

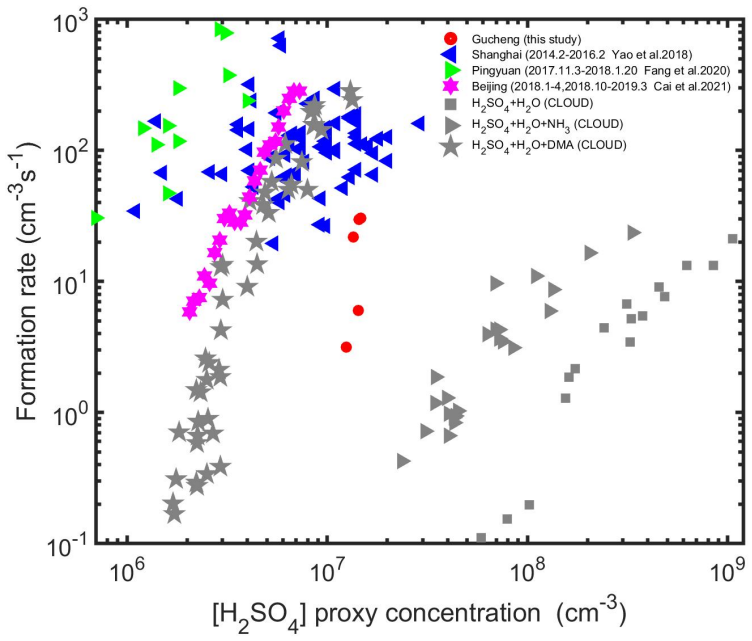

Figure 4. The particle formation rate ($J_{1.3}$) as a function of H_2SO_4 concentration for our study as well as for urban Shanghai (Yao et al., 2018), Beijing (Cai et al., 2021b), rural Pingyuan (Fang et al., 2020) and CLOUD measurements. Gray square, triangle, pentagram, and diamond represents the CLOUD data for H_2SO_4+H_2O, H_2SO_4+H_2O+NH_3, H_2SO_4+H_2O+DMA (Kirkby et al. (2011) and Riccobono et al. (2014)), where DMA represents dimethylamine.

3.3 Governing factors for the occurrence of NPF in rural NCP

The high concentration of SO_2, NH_3, NO_X, VOCs (Chu et al., 2019) as well as fine particles makes the NCP of China an unique condition for NPF compared to many other environments. In principle, the competition between how fast the

设置格式[洪娟]: 字体: （默认）Calibri, 小四, 非倾斜
删除[洪娟]: However, by taking into account the contribu
设置格式[洪娟]: 居中
删除[洪娟]:
删除[Tang Min]: 4
设置格式[洪娟 [2]]: 缩进: 首行缩进: 2 字符
设置格式[洪娟]: 下标
设置格式[洪娟]: 下标
设置格式[洪娟]: 下标
删除[Tang Min]: (Chu et al., 2019)

newly-formed clusters grow and how fast they are scavenged determines whether NPF will occur or not in the atmosphere. However, in the NCP, the concentration of SA was typically quite high, probably reaching its maximum rate to form clusters. Thus, CS or CoagS becomes the dominant factor controlling the occurrence of NPF. This was partly confirmed by existing observations, for instance, Cai et al. (2021) found that H_2SO_4 was high enough in urban Beijing, but not necessarily led to the occurrence of NPF there. They pointed out that as long as CS or CoagS was below a certain threshold (Cai et al., 2017), NPF is very likely take place.

Was this also true for rural atmosphere in the NCP? By comparing with non-event days at our site (see Fig. 5a), we noticed that H_2SO_4 level was not significantly higher but sometimes even lower than that during non-event days. In other words, the abundance of H_2SO_4 did not always lead to NPF; and it was only when CS was significantly lowered that the event became more likely to occur. This strongly demonstrates the similarity between our site with urban Beijing, that CS would be the limiting factor for the occurrence of NPF. However, we noticed that there were a very few cases (two cases) that CS was somewhat quite low, being quite close to that under those event days, yet NPF still did not occur. The most plausible explanation for this could be on the one hand the lowered H_2SO_4 concentration at these days (as shown in Fig. 5a) and on the other hand the other nucleating species rather than H_2SO_4 may not be always enough to initiate nucleation at this site.

As previously stated that the dimensionless criterion, *I*, is a good quantitative indicator to predict whether an NPF occurs or not during a certain day, we plotted *I* against the condensational sink for NPF days and other days under different H_2SO_4 level. Cai et al. (2021) found that the larger the *I* value, the higher frequency that NPF events occurred for both urban Beijing and Shanghai, which was also clearly revealed by our results. On the one hand, as shown in Fig. 5b, the largest *I* values were mostly observed for NPF days, confirming its feasibility in predicting the occurrence of NPF events. On the other hand, the obtained *I* anti-correlated with CS quite well, while the influence from the available H_2SO_4 was not obvious. This

设置格式[洪娟]: 下标
设置格式[洪娟]: 下标
删除[洪娟 [2]]:
删除[洪娟]:
删除[洪娟 [2]]:
删除[洪娟]: Was this also true for rural atmosphere in the NCP? By comparing with event days at our site, we noticed that CS level was in general higher during non-event days.
设置格式[洪娟]: 字体: 小四
设置格式[洪娟]: 突出显示
设置格式[洪娟]: 突出显示
设置格式[洪娟]: 突出显示
设置格式[洪娟]: 突出显示
设置格式[洪娟]: 突出显示
设置格式[洪娟]: 突出显示
设置格式[洪娟 [2]]: 缩进: 首行缩进: 2 字符, 行距: 1.5 倍行距
设置格式[洪娟]: 突出显示
设置格式[洪娟]: 突出显示
设置格式[洪娟]: 突出显示
设置格式[洪娟]: 字体: （默认）Calibri, 小四, 非倾斜
设置格式[洪娟]: 字体: （默认）Calibri, 小四, 非倾斜, 下标
设置格式[洪娟]: 字体: （默认）Calibri, 小四, 非倾斜
设置格式[洪娟]: 字体: （默认）Calibri, 小四, 非倾斜, 下标
设置格式[洪娟]: 字体: （默认）Calibri, 小四, 非倾斜
删除[洪娟 [2]]:
设置格式[洪娟]: 字体: （默认）Calibri, 小四, 非倾斜
设置格式[洪娟 [2]]: 缩进: 首行缩进: 2 字符

434 strongly suggests that CS was the dominating factor governing the appearance of
435 NPF events at current environment, being highly consistent with the feature in
436 Beijing.

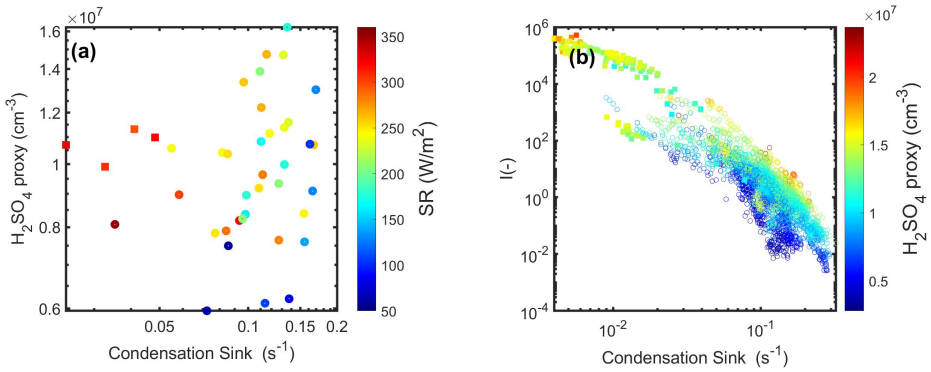

437
438 Figure 5. (a) H_2SO_4 concentration as a function of condensation sink during both event days
439 (squares) and no-event days (circular dots) during our study. (b) The dimensionless indicator, *I*, as
440 a function of the condensational sink. The colorbar indicates: solar radiation (left panel) and
441 H_2SO_4 proxy concentration (right panel).

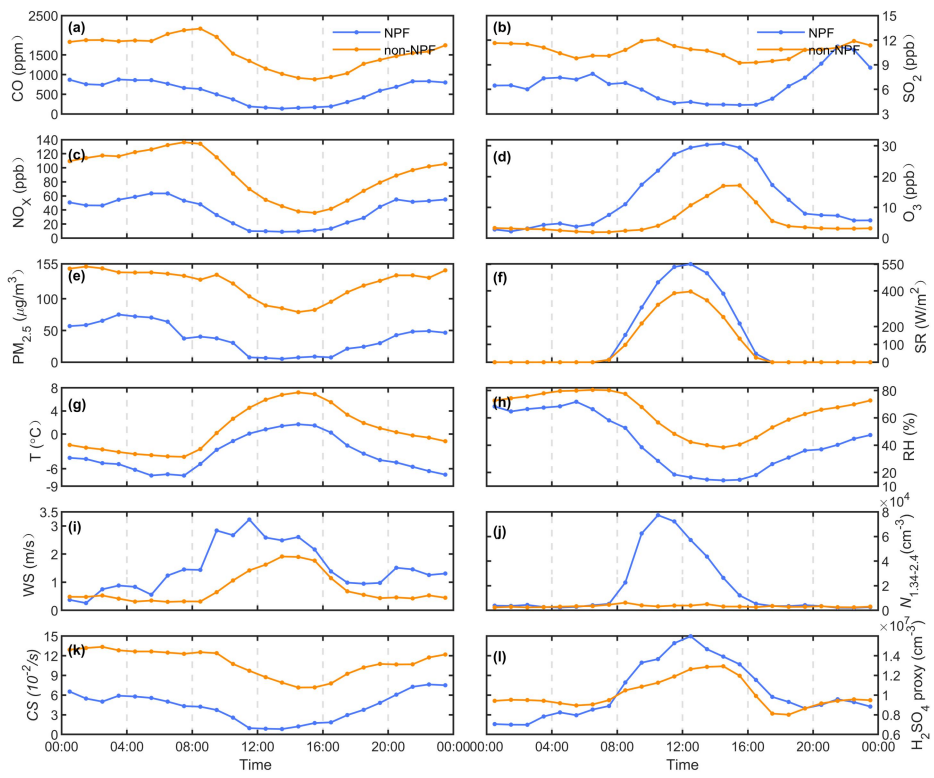

442
443 **Figure 6.** Diurnal variation of (a) CO, (b) SO_2, (c) NO_x, (d) O_3, (e) $PM_{2.5}$, (f) Solar radiation (SR), (g) *T*,
444 (h) RH, (i) wind speed (WS), (j) number concentration of sub-3nm cluster, (k) *CS*, and (l) H_2SO_4
445 proxy during the NPF and non-NPF days during this field campaign. These values were
446 averaged over the five NPF days and 28 non-event days, respectively.

设置格式[洪娟]: 字体: （默认）Calibri
设置格式[洪娟]: 字体: （默认）Calibri, 倾斜
设置格式[洪娟]: 字体: （默认）Calibri
设置格式[洪娟]: 字体: （默认）Calibri
设置格式[洪娟]: 字体: （默认）Calibri
删除[洪娟 [2]]:
删除[洪娟]:
设置格式[洪娟 [2]]: 行距: 单倍行距

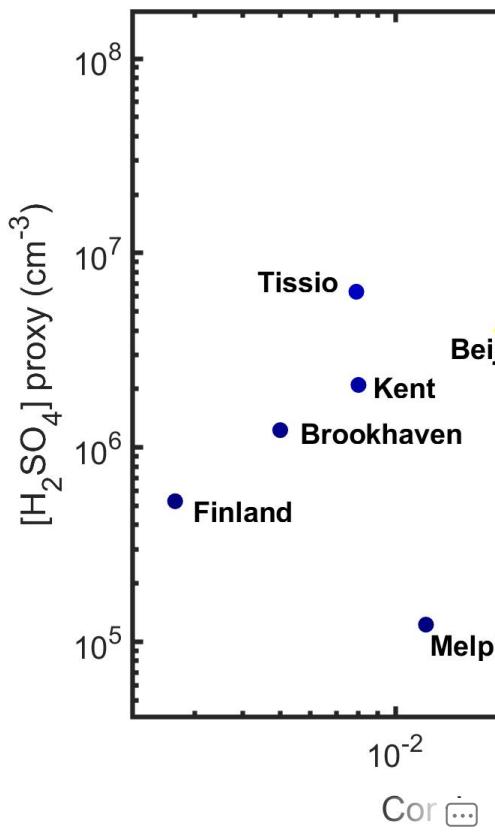

删除[洪娟]:

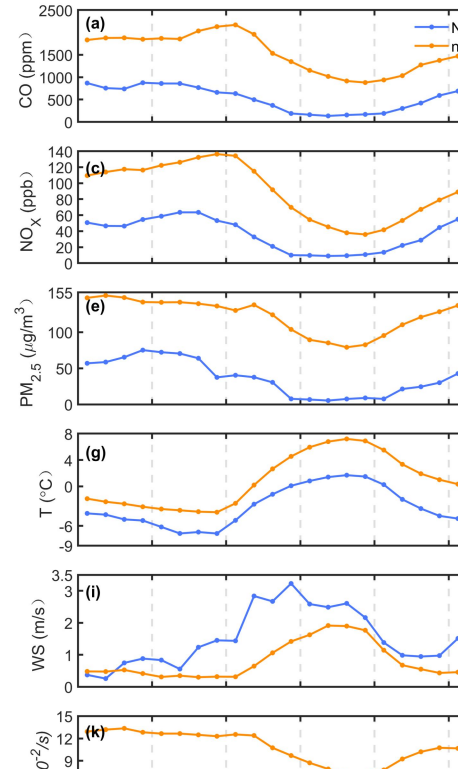

On the other hand, we found that RH level under event days was generally lower than that on non-event days (see Fig. 6). This is similar to the cases that NPF was observed in Beijing by Yue et al. (2009), who suggested that photochemical reactions were faster on sunny days with low RH. In addition to this, ambient temperature during NPF was relatively lower than that on non-event days (Kirkby et al. (2011);Riccobono et al. (2014)). Yan et al. (2021) considered that temperature can affect the stability of H_2SO_4 clustering and thus influence NPF. Therefore, all these factors could be the potential reasons increase or decrease the probability of NPF to occur in current rural areas. It has to be noted that all these features, including reduced RH level as well as ambient *T* during event days, could be coincidence with reduced CS over clean days, for instance, being a consequence of air masses originating from the north and bringing dryer, colder and cleaner air to the site. Therefore, current discussion in this regard becomes ambiguous and may be inclusive, but should still be considered separately when larger datasets are available. Moreover, we observed that O_3 concentration was clearly higher during event days, implying that other condensable vapors, for instance, organics, that involve O_3, among others, in forming HOM, might also be important to NPF in this region. Although these organic compounds formed through O_3 oxidation (Mohr et al., 2019) may not necessarily participate in H_2SO_4 clustering, they may considerably contribute to the growth of newly-formed particles, which should not be ruled out in the study of NPF for this region and also need to be investigated in the future.

4. Summary and conclusions

Most previous studies dealing with NPF in China were mainly based on measurements of particles at larger sizes, typically above 3 nm, whereas detection of particles at sub-3 nm range was quite limited. In our study, by coupling a PSM with a traditional SMPS, We were able to measure the particle number size distribution down to 1.3 nm during NPF events in the wintertime at a rural site of the NCP. Correspondingly, formation rate of particles at 1.3 nm was obtained, widening the

删除[洪娟 [2]]:
设置格式[洪娟 [2]]: 缩进: 首行缩进: 2 字符
删除[Tang Min]: (
删除[Tang Min]: .,
设置格式[洪娟]: 非突出显示
删除[Tang Min]: (
删除[Tang Min]: ,
设置格式[洪娟]: 下标
设置格式[洪娟]: 下标
设置格式[洪娟]: 字体: （默认）Calibri, 小四, 非倾斜
删除[洪娟]: Moreover, we observed that O_3 concentration was clearly higher during event days, implying that other condensable vapours, for instance, organics, that involve O3, OH, NO3 are oxidants involved in forming HOM that involving O_3 oxidation, might also be important to NPF in this region.
设置格式[Tang Min]: 突出显示
设置格式[Tang Min]: 突出显示
设置格式[洪娟]: 字体: （默认）Calibri, 小四, 非倾斜
删除[Juan Hong]: (Mohr et al., 2019)
设置格式[洪娟]: 字体: （默认）Calibri, 小四, 非倾斜
删除[洪娟]: oxygenated organic compounds
设置格式[洪娟]: 下标
设置格式[洪娟]: 下标
设置格式[洪娟 [2]]: 缩进: 首行缩进: 2 字符
删除[Tang Min]: 4
删除[Tang Min]: 4

data pool concerning the feature of NPF for this region. At current rural environment, high level of H_2SO_4 may not always initiate the occurrence of NPF. Only at the condition that the CS was considerably low, NPF events were more likely to take place. This feature is quite similar to that of the urban atmosphere of NCP, whereas NPF events were usually characterized with high formation rates, high CS and high H_2SO_4 concentration. However, as our H_2SO_4 concentration was predicted from empirical parameters, particular cautions regarding their associated uncertainties should be considered. Yang et al. (2021) demonstrated that the derived fitting parameters for the calculations of H_2SO_4 proxy may vary from site to site and between different seasons. For instance, they considered the products from the ozonolysis of alkenes were able to oxidize SO_2 to form gaseous H_2SO_4. Moreover, they pointed out that H_2SO_4 could be from primary emissions, such as vehicles or freshly emitted plumes. Sulfuric acid from these sources could account for 10% of the total H_2SO_4 in the atmosphere. These aspects were not comprehensively considered in our calculations, which could bring huge uncertainties or errors to the estimation. Thereby, direct measurements for the H_2SO_4 concentration should be implemented in the future before driving any further conclusion.

设置格式[洪娟]: 下标

设置格式[洪娟]: 下标

删除[洪娟]: or low concentration of fine particles

删除[洪娟]: concentration of H2SO4 was relatively high and

删除[洪娟]: slightly different from

设置格式[洪娟]: 下标

设置格式[洪娟]: 下标

设置格式[洪娟]: 下标

设置格式[洪娟]: 下标

删除[洪娟]: At urban Beijing, NPF was also observed during the wintertime of 2018. We found that their measured H_2SO_4 concentration was quite comparable to the predicted ones in our study, indicating its relative reliability in using them though absolute uncertainties could not be derived here.

设置格式[洪娟]: 下标

设置格式[洪娟]: 下标

设置格式[洪娟]: 字体: （默认）Calibri, 小四, 非倾斜

设置格式[洪娟]: 字体: （默认）Calibri, 小四, 非倾斜

删除[洪娟]: Moreover, they pointed out that H_2SO_4 could be from primary emissions, such as vehicles, or freshly emitted plumes, . H_2SO_4 from primary emissionswhich could account for 10% of the total H_2SO_4 in the atmosphere.

设置格式[洪娟]: 突出显示

删除[洪娟]: , though the H_2SO_4 proxy was approximated to the measured ones at Beijing site,

删除[洪娟]:

Declaration of interest statement.

The authors declare that they have no known competing financial interests or personal relationships that could have appeared to influence the work reported in this paper.

Data availability.

The details data can be obtained from https://doi.org/10.5281/zenodo.7326388 (Hong, 2022).

Author contributions.

JH collected the resources, wrote and finalized the manuscript, MT analyzed the data, plotted the figures and wrote the original draft, QQW and NM planned the study, collected the resources, reviewed the manuscript. SWZ, SBZ, XHP, LHX, GL, UK conducted the measurements, CY, JCT, YK, YH, YQZ, WYX, GSZ, BY, ZBW discussed the results. YFC and HS contributed to fund acquisition.

Competing interests.

Hang Su and Yafang Cheng are members of the editorial board of Atmospheric Chemistry and Physics

Acknowledgements.

This work is supported by the National Natural Science Foundation of China (grant no. 42175117, 41907182, 41877303, 91644218) and the National key R&D Program of China (2018YFC0213901), the Fundamental Research Funds for the Central Universities (21621105), the Guangdong Innovative and Entrepreneurial Research Team Program (Research team on atmospheric environmental roles and effects of carbonaceous species: 2016ZT06N263), and Special Fund Project for Science and Technology Innovation Strategy of Guangdong Province (2019B121205004).

删除[洪娟]:

删除[洪娟 [2]]:

References

Almeida, J., Schobesberger, S., Kürten, A., Ortega, I. K., Kupiainen-Määttä, O., Praplan, A. P., Adamov, A., Amorim, A., Bianchi, F., Breitenlechner, M., David, A., Dommen, J., Donahue, N. M., Downard, A., Dunne, E., Duplissy, J., Ehrhart, S., Flagan, R. C., Franchin, A., Guida, R., Hakala, J., Hansel, A., Heinritzi, M., Henschel, H., Jokinen, T., Junninen, H., Kajos, M., Kangasluoma, J., Keskinen, H., Kupc, A., Kurtén, T., Kvashin, A. N., Laaksonen, A., Lehtipalo, K., Leiminger, M., Leppä, J., Loukonen, V., Makhmutov, V., Mathot, S., McGrath, M. J., Nieminen, T., Olenius, T., Onnela, A., Petäjä, T., Riccobono, F., Riipinen, I., Rissanen, M., Rondo, L., Ruuskanen, T., Santos, F. D., Sarnela, N., Schallhart, S., Schnitzhofer, R., Seinfeld, J. H., Simon, M., Sipilä, M., Stozhkov, Y., Stratmann, F., Tomé, A., Tröstl, J., Tsagkogeorgas, G., Vaattovaara, P., Viisanen, Y., Virtanen, A., Vrtala, A., Wagner, P. E., Weingartner, E., Wex, H., Williamson, C., Wimmer, D., Ye, P., Yli-Juuti, T., Carslaw, K. S., Kulmala, M., Curtius, J., Baltensperger, U., Worsnop, D. R., Vehkamäki, H., and Kirkby, J.: Molecular understanding of sulphuric acid-amine particle nucleation in the atmosphere, Nature, 502, 359–363, https://doi.org/10.1038/nature12663, 2013.

Baalbaki, R., Pikridas, M., Jokinen, T., Laurila, T., Dada, L., Bezantakos, S., Ahonen, L., Neitola, K., Maisser, A., Bimenyimana, E., Christodoulou, A., Unga, F., Savvides, C., Lehtipalo, K., Kangasluoma, J., Biskos, G., Petäjä, T., Kerminen, V.-M., Sciare, J., and Kulmala, M.: Towards understanding the mechanisms of new particle formation in the Eastern Mediterranean, Atmos. Chem. Phys. Discuss., 1–44, https://doi.org/10.5194/acp-2020-1066, 2020.

Berndt, T., Stratmann, F., Sipilä, M., Vanhanen, J., Petäjä, T., Mikkilä, J., Grüner, A., Spindler, G., Lee Mauldin, R., Curtius, J., Kulmala, M., and Heintzenberg, J.: Laboratory study on new particle formation from the reaction OH + SO2: Influence of experimental conditions, H2O vapour, NH3 and the amine tert-butylamine on the overall process, Atmos. Chem. Phys., 10, 7101–7116, https://doi.org/10.5194/acp-10-7101-2010, 2010.

Bianchi, F., Tröstl, J., Junninen, H., Frege, C., Henne, S., Hoyle, C. R., Molteni, U., Herrmann, E., Adamov, A., Bukowiecki, N., Chen, X., Duplissy, J., Gysel, M., Hutterli, M., Kangasluoma, J., Kontkanen, J., Kürten, A., Manninen, H. E., Münch, S., Peräkylä, O., Petäjä, T., Rondo, L., Williamson, C., Weingartner, E., Curtius, J., Worsnop, D. R., Kulmala, M., Dommen, J., and Baltensperger, U.: New particle formation in the free troposphere: A question of chemistry and timing, Science (80-.)., 352, 1109–1112, https://doi.org/10.1126/science.aad5456, 2016.

Boulon, J., Sellegri, K., Venzac, H., Picard, D., Weingartner, E., Wehrle, G., Collaud Coen, M., Bütikofer, R., Flückiger, E., Baltensperger, U., and Laj, P.: New particle formation and ultrafine charged aerosol climatology at a high altitude site in the Alps (Jungfraujoch, 3580 m a.s.l., Switzerland), Atmos. Chem. Phys., 10, 9333–9349, https://doi.org/10.5194/acp-10-9333-2010, 2010.

Cai, R. and Jiang, J.: A new balance formula to estimate new particle formation rate: Reevaluating the effect of coagulation scavenging, Atmos. Chem. Phys., 17, 12659–12675, https://doi.org/10.5194/acp-17-12659-2017, 2017.

Cai, R., Yang, D., Fu, Y., Wang, X., Li, X., Ma, Y., Hao, J., Zheng, J., and Jiang, J.: Aerosol surface area concentration: A governing factor in new particle formation in Beijing, Atmos. Chem. Phys., 17, 12327–12340, https://doi.org/10.5194/acp-17-12327-2017, 2017.

设置格式[洪娟 [2]]: 两端对齐

设置格式[洪娟 [2]]: 字体: 五号

Cai, R., Yan, C., Worsnop, D. R., Bianchi, F., Kerminen, V.-M., Liu, Y., Wang, L., Zheng, J., Kulmala, M., and Jiang, J.: An indicator for sulfuric acid–amine nucleation in atmospheric environments, Aerosol Sci. Technol., 55, 1059–1069, https://doi.org/10.1080/02786826.2021.1922598, 2021a.

Cai, R., Yan, C., Yang, D., Yin, R., Lu, Y., Deng, C., Fu, Y., Ruan, J., Li, X., Kontkanen, J., Zhang, Q., Kangasluoma, J., Ma, Y., Hao, J., Worsnop, D. R., Bianchi, F., Paasonen, P., Kerminen, V. M., Liu, Y., Wang, L., Zheng, J., Kulmala, M., and Jiang, J.: Sulfuric acid-amine nucleation in urban Beijing, Atmos. Chem. Phys., 21, 2457–2468, https://doi.org/10.5194/acp-21-2457-2021, 2021b.

CHEN Chen, HU Min, WU Zhi-jun, WU Yu-sheng, GUO Song, CHEN Wen-tai, LUO Bin, SHAO Min, ZHANG Yuan-hang, X. S.: Characterization of new particle formation event in the rural site of Sichuan Basin and its contribution to cloud condensation nuclei., China Environ. Sci., 34, 2764–2772, 2014.

Chu, B., Matti Kerminen, V., Bianchi, F., Yan, C., Petäjä, T., and Kulmala, M.: Atmospheric new particle formation in China, Atmos. Chem. Phys., 19, 115–138, https://doi.org/10.5194/acp-19-115-2019, 2019.

Chu, B., Dada, L., Liu, Y., Yao, L., Wang, Y., Du, W., Cai, J., Dällenbach, K. R., Chen, X., Simonen, P., Zhou, Y., Deng, C., Fu, Y., Yin, R., Li, H., He, X. C., Feng, Z., Yan, C., Kangasluoma, J., Bianchi, F., Jiang, J., Kujansuu, J., Kerminen, V. M., Petäjä, T., He, H., and Kulmala, M.: Particle growth with photochemical age from new particle formation to haze in the winter of Beijing, China, Sci. Total Environ., 753, 142207, https://doi.org/10.1016/j.scitotenv.2020.142207, 2021.

Dal Maso, M., Kulmala, M., Riipinen, I., Wagner, R., Hussein, T., Aalto, P. P., and Lehtinen, K. E. J.: Formation and growth of fresh atmospheric aerosols: Eight years of aerosol size distribution data from SMEAR II, Hyytiälä, Finland, Boreal Environ. Res., 10, 323–336, 2005.

Deng, C., Fu, Y., Dada, L., Yan, C., Cai, R., Yang, D., Zhou, Y., Yin, R., Lu, Y., Li, X., Qiao, X., Fan, X., Nie, W., Kontkanen, J., Kangasluoma, J., Chu, B., Ding, A., Kerminen, V.-M., Paasonen, P., Worsnop, D. R., Bianchi, F., Liu, Y., Zheng, J., Wang, L., Kulmala, M., and Jiang, J.: Seasonal Characteristics of New Particle Formation and Growth in Urban Beijing, Environ. Sci. Technol., acs.est.0c00808, https://doi.org/10.1021/acs.est.0c00808, 2020.

Dunne, E. M., Gordon, H., Kürten, A., Almeida, J., Duplissy, J., Williamson, C., Ortega, I. K., Pringle, K. J., Adamov, A., Baltensperger, U., Barmet, P., Benduhn, F., Bianchi, F., Breitenlechner, M., Clarke, A., Curtius, J., Dommen, J., Donahue, N. M., Ehrhart, S., Flagan, R. C., Franchin, A., Guida, R., Hakala, J., Hansel, A., Heinritzi, M., Jokinen, T., Kangasluoma, J., Kirkby, J., Kulmala, M., Kupc, A., Lawler, M. J., Lehtipalo, K., Makhmutov, V., Mann, G., Mathot, S., Merikanto, J., Miettinen, P., Nenes, A., Onnela, A., Rap, A., Reddington, C. L. S., Riccobono, F., Richards, N. A. D., Rissanen, M. P., Rondo, L., Sarnela, N., Schobesberger, S., Sengupta, K., Simon, M., Sipilä, M., Smith, J. N., Stozkhov, Y., Tomé, A., Tröstl, J., Wagner, P. E., Wimmer, D., Winkler, P. M., Worsnop, D. R., and Carslaw, K. S.: Global atmospheric particle formation from CERN CLOUD measurements, Science (80-.)., 354, 1119–1124, https://doi.org/10.1126/science.aaf2649, 2016.

Ehn, M., Thornton, J. A., Kleist, E., Sipilä, M., Junninen, H., Pullinen, I., Springer, M., Rubach, F., Tillmann, R., Lee, B., Lopez-Hilfiker, F., Andres, S., Acir, I.-H., Rissanen, M., Jokinen, T., Schobesberger, S., Kangasluoma, J., Kontkanen, J., Nieminen, T., Kurtén, T., Nielsen, L. B., Jørgensen, S., Kjaergaard, H. G., Canagaratna, M., Maso, M. D., Berndt, T., Petäjä, T., Wahner, A., Kerminen, V.-M., Kulmala, M., Worsnop, D. R., Wildt, J., and Mentel, T. F.: A large source of low-volatility secondary organic aerosol., Nature, 506, 476–9, https://doi.org/10.1038/nature13032, 2014.

Fang, X., Hu, M., Shang, D., Tang, R., Shi, L., Olenius, T., Wang, Y., Wang, H., Zhang, Z., Chen, S., Yu, X., Zhu, W., Lou, S., Ma, Y., Li, X., Zeng, L., Wu, Z., Zheng, J., and Guo, S.: Observational Evidence for the Involvement of Dicarboxylic Acids in Particle Nucleation, Environ. Sci. Technol. Lett., https://doi.org/10.1021/acs.estlett.0c00270, 2020.

Guo, H., Wang, D. W., Cheung, K., Ling, Z. H., Chan, C. K., and Yao, X. H.: Observation of aerosol size distribution and new particle formation at a mountain site in subtropical Hong Kong, Atmos. Chem. Phys., 12, 9923–9939, https://doi.org/10.5194/acp-12-9923-2012, 2012.

Guo, S., Hu, M., Zamora, M. L., Peng, J., Shang, D., Zheng, J., Du, Z., Wu, Z., Shao, M., Zeng, L., Molina, M. J., and Zhang, R.: Elucidating severe urban haze formation in China, Proc. Natl. Acad. Sci. U. S. A., 111, 17373–17378, https://doi.org/10.1073/pnas.1419604111, 2014.

Hamed, A., Birmili, W., Joutsensaari, J., Mikkonen, S., Asmi, A., Wehner, B., Spindler, G., Jaatinen, A., Wiedensohler, A., Korhonen, H., J. Lehtinen, K. E., and Laaksonen, A.: Changes in the production rate of secondary aerosol particles in Central Europe in view of decreasing SO2 emissions between 1996 and 2006, Atmos. Chem. Phys., 10, 1071–1091, https://doi.org/10.5194/acp-10-1071-2010, 2010.

Herrmann, E., Ding, A. J., Kerminen, V. M., Petäjä, T., Yang, X. Q., Sun, J. N., Qi, X. M., Manninen, H., Hakala, J., Nieminen, T., Aalto, P. P., Kulmala, M., and Fu, C. B.: Aerosols and nucleation in eastern China: First insights from the new SORPES-NJU station, Atmos. Chem. Phys., 14, 2169–2183, https://doi.org/10.5194/acp-14-2169-2014, 2014.

Hussein, T., Dal Maso, M., Petäjä, T., Koponen, I. K., Paatero, P., Aalto, P. P., Hämeri, K., and Kulmala, M.: Evaluation of an automatic algorithm for fitting the particle number size distributions, Boreal Environ. Res., 10, 337–355, 2005.

Jokinen, T., Sipilä, M., Junninen, H., Ehn, M., Lönn, G., Hakala, J., Petäjä, T., Mauldin, R. L., Kulmala, M., and Worsnop, D. R.: Atmospheric sulphuric acid and neutral cluster measurements using CI-APi-TOF, Atmos. Chem. Phys., 12, 4117–4125, https://doi.org/10.5194/acp-12-4117-2012, 2012.

Kalkavouras, P., Bougiatioti, A., Grivas, G., Stavroulas, I., Kalivitis, N., Liakakou, E., Gerasopoulos, E., Pilinis, C., and Mihalopoulos, N.: On the regional aspects of new particle formation in the Eastern Mediterranean: A comparative study between a background and an urban site based on long term observations, Atmos. Res., 239, 104911, https://doi.org/10.1016/j.atmosres.2020.104911, 2020.

Kirkby, J., Curtius, J., Almeida, J., Dunne, E., Duplissy, J., Ehrhart, S., Franchin, A., Gagné, S., Ickes, L., Kürten, A., Kupc, A., Metzger, A., Riccobono, F., Rondo, L., Schobesberger, S., Tsagkogeorgas, G., Wimmer, D., Amorim, A., Bianchi, F., Breitenlechner, M., David, A., Dommen, J., Downard, A., Ehn, M., Flagan, R. C., Haider, S., Hansel, A., Hauser, D., Jud, W., Junninen, H., Kreissl, F., Kvashin, A., Laaksonen, A., Lehtipalo, K., Lima, J., Lovejoy, E. R., Makhmutov, V., Mathot, S., Mikkilä, J., Minginette, P., Mogo, S., Nieminen, T., Onnela, A., Pereira, P., Petäjä, T., Schnitzhofer, R., Seinfeld, J. H., Sipilä, M., Stozhkov, Y., Stratmann, F., Tomé, A., Vanhanen, J., Viisanen, Y., Vrtala, A., Wagner, P. E., Walther, H., Weingartner, E., Wex, H., Winkler, P. M., Carslaw, K. S., Worsnop, D. R., Baltensperger, U., and Kulmala, M.: Role of sulphuric acid, ammonia and galactic cosmic rays in atmospheric aerosol nucleation, Nature, 476, 429–435, https://doi.org/10.1038/nature10343, 2011.

Kirkby, J., Duplissy, J., Sengupta, K., Frege, C., Gordon, H., Williamson, C., Heinritzi, M., Simon, M., Yan, C., Almeida, J., Trostl, J., Nieminen, T., Ortega, I. K., Wagner, R., Adamov, A., Amorim, A.,

Bernhammer, A. K., Bianchi, F., Breitenlechner, M., Brilke, S., Chen, X., Craven, J., Dias, A., Ehrhart, S., Flagan, R. C., Franchin, A., Fuchs, C., Guida, R., Hakala, J., Hoyle, C. R., Jokinen, T., Junninen, H., Kangasluoma, J., Kim, J., Krapf, M., Kurten, A., Laaksonen, A., Lehtipalo, K., Makhmutov, V., Mathot, S., Molteni, U., Onnela, A., Perakyla, O., Piel, F., Petaja, T., Praplan, A. P., Pringle, K., Rap, A., Richards, N. A. D., Riipinen, I., Rissanen, M. P., Rondo, L., Sarnela, N., Schobesberger, S., Scott, C. E., Seinfeld, J. H., Sipila, M., Steiner, G., Stozhkov, Y., Stratmann, F., Tomé, A., Virtanen, A., Vogel, A. L., Wagner, A. C., Wagner, P. E., Weingartner, E., Wimmer, D., Winkler, P. M., Ye, P., Zhang, X., Hansel, A., Dommen, J., Donahue, N. M., Worsnop, D. R., Baltensperger, U., Kulmala, M., Carslaw, K. S., and Curtius, J.: Ion-induced nucleation of pure biogenic particles, Nature, 533, 521–526, https://doi.org/10.1038/nature17953, 2016.

Kompalli, S. K., Nair, V. S., Jayachandran, V., Gogoi, M. M., and Babu, S. S.: Particle number size distributions and new particle formation events over the northern Indian Ocean during continental outflow, Atmos. Environ., 238, 117719, https://doi.org/10.1016/j.atmosenv.2020.117719, 2020.

Kuang, C., Riipinen, I., Sihto, S.-L., Kulmala, M., McCormick, A. V., and McMurry, P. H.: An improved criterion for new particle formation in diverse atmospheric environments, Atmos. Chem. Phys., 10, 8469–8480, https://doi.org/10.5194/acp-10-8469-2010, 2010.

Kulmala, M.: Direct Observations of Atmospheric Aerosol Nucleation, Science (80-.)., 943, https://doi.org/10.1126/science.1227385, 2013.

Kulmala, M., Pirjola, L., and Mäkelä, J. M.: Stable sulphate clusters as a source of new atmospheric particles, Nature, 404, 66–69, https://doi.org/10.1038/35003550, 2000.

Kulmala, M., Vehkamäki, H., Petäjä, T., Dal Maso, M., Lauri, A., Kerminen, V. M., Birmili, W., and McMurry, P. H.: Formation and growth rates of ultrafine atmospheric particles: A review of observations, J. Aerosol Sci., 35, 143–176, https://doi.org/10.1016/j.jaerosci.2003.10.003, 2004.

Kulmala, M., Petäjä, T., Nieminen, T., Sipilä, M., Manninen, H. E., Lehtipalo, K., Dal Maso, M., Aalto, P. P., Junninen, H., Paasonen, P., Riipinen, I., Lehtinen, K. E. J., Laaksonen, A., and Kerminen, V.-M.: Measurement of the nucleation of atmospheric aerosol particles, Nat. Protoc., 7, 1651–1667, https://doi.org/10.1038/nprot.2012.091, 2012.

Kulmala, M., Petäjä, T., Ehn, M., Thornton, J., Sipilä, M., Worsnop, D. R., and Kerminen, V. M.: Chemistry of atmospheric nucleation: On the recent advances on precursor characterization and atmospheric cluster composition in connection with atmospheric new particle formation, Annu. Rev. Phys. Chem., 65, 21–37, https://doi.org/10.1146/annurev-physchem-040412-110014, 2014.

Kulmala, M., Kerminen, V.-M., Petäjä, T., Ding, A. J., and Wang, L.: Atmospheric gas-to-particle conversion: why NPF events are observed in megacities?, Faraday Discuss., 200, 271–288, https://doi.org/10.1039/C6FD00257A, 2017.

Kulmama, M., Petäjä, T., Kerminen, V. M., Kujansuu, J., Ruuskanen, T., Ding, A., Nie, W., Hu, M., Wang, Z., Wu, Z., Wang, L., and Worsnop, D. R.: On secondary new particle formation in China, Front. Environ. Sci. Eng., 10, 1–10, https://doi.org/10.1007/s11783-016-0850-1, 2016.

Kürten, A., Bergen, A., Heinritzi, M., Leiminger, M., Lorenz, V., Piel, F., Simon, M., Sitals, R., Wagner, A. C., and Curtius, J.: Observation of new particle formation and measurement of sulfuric acid, ammonia, amines and highly oxidized organic molecules at a rural site in central Germany, Atmos. Chem. Phys., 16, 12793–12813, https://doi.org/10.5194/acp-16-12793-2016, 2016.

Lin, W., Xu, X., Ge, B., and Zhang, X.: Characteristics of gaseous pollutants at Gucheng, a rural site

southwest of Beijing, J. Geophys. Res. Atmos., 114, https://doi.org/10.1029/2008JD010339, 2009.
Liu, S., Hu, M., Wu, Z., Wehner, B., Wiedensohler, A., and Cheng, Y.: Aerosol number size distribution and new particle formation at a rural/coastal site in Pearl River Delta (PRD) of China, Atmos. Environ., 42, 6275–6283, https://doi.org/10.1016/j.atmosenv.2008.01.063, 2008.
Liu, Y., Yan, C., Feng, Z., Zheng, F., Fan, X., Zhang, Y., Li, C., Zhou, Y., Lin, Z., Guo, Y., Zhang, Y., Ma, L., Zhou, W., Liu, Z., Dada, L., Dällenbach, K., Kontkanen, J., Cai, R., Chan, T., Chu, B., Du, W., Yao, L., Wang, Y., Cai, J., Kangasluoma, J., Kokkonen, T., Kujansuu, J., Rusanen, A., Deng, C., Fu, Y., Yin, R., Li, X., Lu, Y., Liu, Y., Lian, C., Yang, D., Wang, W., Ge, M., Wang, Y., Worsnop, D. R., Junninen, H., He, H., Kerminen, V. M., Zheng, J., Wang, L., Jiang, J., Petäjä, T., Bianchi, F., and Kulmala, M.: Continuous and comprehensive atmospheric observations in Beijing: a station to understand the complex urban atmospheric environment, Big Earth Data, 4, 295–321, https://doi.org/10.1080/20964471.2020.1798707, 2020.
Lu, Y., Yan, C., Fu, Y., Chen, Y., Liu, Y., Yang, G., Wang, Y., Bianchi, F., Chu, B., Zhou, Y., Yin, R., Baalbaki, R., Garmash, O., Deng, C., Wang, W., Liu, Y., Petäjä, T., Kerminen, V. M., Jiang, J., Kulmala, M., and Wang, L.: A proxy for atmospheric daytime gaseous sulfuric acid concentration in urban Beijing, Atmos. Chem. Phys., 19, 1971–1983, https://doi.org/10.5194/acp-19-1971-2019, 2019.
Ma, N., Zhao, C., Tao, J., Wu, Z., Kecorius, S., Wang, Z., Groß, J., Liu, H., Bian, Y., Kuang, Y., Teich, M., Spindler, G., Muller, K., Van Pinxteren, D., Herrmann, H., Hu, M., and Wiedensohler, A.: Variation of CCN activity during new particle formation events in the North China Plain, Atmos. Chem. Phys., 16, 8593–8607, https://doi.org/10.5194/acp-16-8593-2016, 2016.
McMurry, P. H., Fink, M., Sakurai, H., Stolzenburg, M. R., Mauldin, I. L., Smith, J., Eisele, F., Moore, K., Sjostedt, S., Tanner, D., Huey, L. G., Nowak, J. B., Edgerton, E., and Voisin, D.: A criterion for new particle formation in the sulfur-rich Atlanta atmosphere, J. Geophys. Res. Atmos., 110, 1–10, https://doi.org/10.1029/2005JD005901, 2005.
Mikko Sipilä, Torsten Berndt,Tuukka Petäjä, David Brus, Joonas Vanhanen , Frank Stratmann,Johanna Patokoski, Roy L. Mauldin III, Antti-Pekka HyvärinenFrank Stratmann, Johanna Patokoski, Roy L. Mauldin III, Heikki Lihavainen, M. K.: The Role of Sulfuric Acid in Atmospheric Nucleation, Science (80-.)., 327, 1243–1246, 2010.
Mirme, S. and Mirme, A.: The mathematical principles and design of the NAIS - A spectrometer for the measurement of cluster ion and nanometer aerosol size distributions, Atmos. Meas. Tech., 6, 1061–1071, https://doi.org/10.5194/amt-6-1061-2013, 2013.
Mohr, C., Thornton, J. A., Heitto, A., Lopez-Hilfiker, F. D., Lutz, A., Riipinen, I., Hong, J., Donahue, N. M., Hallquist, M., Petäjä, T., Kulmala, M., and Yli-Juuti, T.: Molecular identification of organic vapors driving atmospheric nanoparticle growth, Nat. Commun., 10, 4442, https://doi.org/10.1038/s41467-019-12473-2, 2019.
Mönkkönen, P., Koponen, I. K., Lehtinen, K. E. J., Hämeri, K., Uma, R., and Kulmala, M.: Measurements in a highly polluted Asian mega city: observations of aerosol number size distribution, modal parameters and nucleation events, Atmos. Chem. Phys. Discuss., 4, 5407–5431, https://doi.org/10.5194/acpd-4-5407-2004, 2005.
Nieminen, T., Lehtinen, K. E. J., and Kulmala, M.: Sub-10 nm particle growth by vapor condensation-effects of vapor molecule size and particle thermal speed, Atmos. Chem. Phys., 10, 9773–9779, https://doi.org/10.5194/acp-10-9773-2010, 2010.

设置格式[洪娟 [2]]: 字体: （默认）Calibri, 五号

设置格式[洪娟 [2]]: 字体: 五号

Nieminen, T., Asmi, A., Aalto, P. P., Keronen, P., Petäjä, T., Kulmala, M., Kerminen, V. M., Nieminen, T., and Dal Maso, M.: Trends in atmospheric new-particle formation: 16 years of observations in a boreal-forest environment, Boreal Environ. Res., 19, 191–214, 2014.

Petäjä, T., Mauldin, R. L., Kosciuch, E., McGrath, J., Nieminen, T., Paasonen, P., Boy, M., Adamov, A., Kotiaho, T., and Kulmala, M.: Sulfuric acid and OH concentrations in a boreal forest site, Atmos. Chem. Phys., 9, 7435–7448, https://doi.org/10.5194/acp-9-7435-2009, 2009.

Riccobono, F., Schobesberger, S., Scott, C. E., Dommen, J., Ortega, I. K., Rondo, L., Almeida, J., Amorim, A., Bianchi, F., Breitenlechner, M., David, A., Downard, A., Dunne, E. M., Duplissy, J., Ehrhart, S., Flagan, R. C., Franchin, A., Hansel, A., Junninen, H., Kajos, M., Keskinen, H., Kupc, A., Kürten, A., Kvashin, A. N., Laaksonen, A., Lehtipalo, K., Makhmutov, V., Mathot, S., Nieminen, T., Onnela, A., Petäjä, T., Praplan, A. P., Santos, F. D., Schallhart, S., Seinfeld, J. H., Sipilä, M., Spracklen, D. V., Stozhkov, Y., Stratmann, F., Tomé, A., Tsagkogeorgas, G., Vaattovaara, P., Viisanen, Y., Vrtala, A., Wagner, P. E., Weingartner, E., Wex, H., Wimmer, D., Carslaw, K. S., Curtius, J., Donahue, N. M., Kirkby, J., Kulmala, M., Worsnop, D. R., and Baltensperger, U.: Oxidation products of biogenic emissions contribute to nucleation of atmospheric particles, Science (80-.)., 344, 717–721, https://doi.org/10.1126/science.1243527, 2014.

Shen, X., Sun, J., Zhang, X., Zhang, Y., Wang, Y., Tan, K., Wang, P., Zhang, L., Qi, X., Che, H., Zhang, Z., Zhong, J., Zhao, H., and Ren, S.: Comparison of Submicron Particles at a Rural and an Urban Site in the North China Plain during the December 2016 Heavy Pollution Episodes, J. Meteorol. Res., 32, 26–37, https://doi.org/10.1007/s13351-018-7060-7, 2018a.

Shen, X., Sun, J., Kivekäs, N., Kristensson, A., Zhang, X., Zhang, Y., Zhang, L., Fan, R., Qi, X., Ma, Q., and Zhou, H.: Spatial distribution and occurrence probability of regional new particle formation events in eastern China, Atmos. Chem. Phys., 18, 587–599, https://doi.org/10.5194/acp-18-587-2018, 2018b.

Spracklen, D. V., Carslaw, K. S., Kulmala, M., Kerminen, V. M., Mann, G. W., and Sihto, S. L.: The contribution of boundary layer nucleation events to total particle concentrations on regional and global scales, Atmos. Chem. Phys., 6, 5631–5648, https://doi.org/10.5194/acp-6-5631-2006, 2006.

Stolzenburg, D., Simon, M., Ranjithkumar, A., Kürten, A., Lehtipalo, K., Gordon, H., Ehrhart, S., Finkenzeller, H., Pichelstorfer, L., Nieminen, T., He, X., Brilke, S., Xiao, M., Amorim, A., Baalbaki, R., Baccarini, A., and Beck, L.: Enhanced growth rate of atmospheric particles from sulfuric acid, 7359–7372, 2020.

Tan, H. B., Yin, Y., Li, F., Liu, X. T., Chan, P. W., Deng, T., Deng, X. J., Wan, Q. L., and Wu, D.: Measurements of particle number size distributions and new particle formation events during winter in the Pearl River Delta region, China, J. Trop. Meteorol., 22, 191–199, https://doi.org/10.16555/j.1006-8775.2016.02.009, 2016.

Tröstl, J., Chuang, W. K., Gordon, H., Heinritzi, M., Yan, C., Molteni, U., Ahlm, L., Frege, C., Bianchi, F., Wagner, R., Simon, M., Lehtipalo, K., Williamson, C., Craven, J. S., Duplissy, J., Adamov, A., Almeida, J., Bernhammer, A. K., Breitenlechner, M., Brilke, S., Dias, A., Ehrhart, S., Flagan, R. C., Franchin, A., Fuchs, C., Guida, R., Gysel, M., Hansel, A., Hoyle, C. R., Jokinen, T., Junninen, H., Kangasluoma, J., Keskinen, H., Kim, J., Krapf, M., Kürten, A., Laaksonen, A., Lawler, M., Leiminger, M., Mathot, S., Möhler, O., Nieminen, T., Onnela, A., Petäjä, T., Piel, F. M., Miettinen, P., Rissanen, M. P., Rondo, L., Sarnela, N., Schobesberger, S., Sengupta, K., Sipilä, M., Smith, J. N., Steiner, G., Tomè, A., Virtanen, A., Wagner, A. C., Weingartner, E., Wimmer, D., Winkler, P. M., Ye, P.,

Carslaw, K. S., Curtius, J., Dommen, J., Kirkby, J., Kulmala, M., Riipinen, I., Worsnop, D. R., Donahue, N. M., and Baltensperger, U.: The role of low-volatility organic compounds in initial particle growth in the atmosphere, Nature, 533, 527–531, https://doi.org/10.1038/nature18271, 2016.

Vanhanen, J., Mikkil, J., Lehtipalo, K., Sipil, M., Manninen, H. E., Siivola, E., and Pet, T.: Particle Size Magnifier for Nano-CN Detection, Aerosol Sci. Technol., 533–542, https://doi.org/10.1080/02786826.2010.547889, 2011.

Varghese, M., Leena, P. P., Murugavel, P., Bankar, S., Todekar, K., Chowdhuri, S., Safai, P. D., Malap, N., Konwar, M., Dixit, S., Rao, Y. J., and Prabha, T. V.: New Particle Formation Observed from a Rain Shadow Region of the Western Ghats India, Toxicol. Environ. Chem., 0, 1–29, https://doi.org/10.1080/02772248.2020.1789134, 2020.

Wang, Z., Wu, Z., Yue, D., Shang, D., Guo, S., Sun, J., Ding, A., Wang, L., Jiang, J., Guo, H., Gao, J., Cheung, H. C., Morawska, L., Keywood, M., and Hu, M.: New particle formation in China: Current knowledge and further directions, Sci. Total Environ., 577, 258–266, https://doi.org/10.1016/j.scitotenv.2016.10.177, 2017.

Wang, Z. B., Hu, M., Sun, J. Y., Wu, Z. J., Yue, D. L., Shen, X. J., Zhang, Y. M., Pei, X. Y., Cheng, Y. F., and Wiedensohler, A.: Characteristics of regional new particle formation in urban and regional background environments in the North China Plain, Atmos. Chem. Phys., 13, 12495–12506, https://doi.org/10.5194/acp-13-12495-2013, 2013.

Xiao, S., Wang, M. Y., Yao, L., Kulmala, M., Zhou, B., Yang, X., Chen, J. M., Wang, D. F., Fu, Q. Y., Worsnop, D. R., and Wang, L.: Strong atmospheric new particle formation in winter in urban Shanghai, China, Atmos. Chem. Phys., 15, 1769–1781, https://doi.org/10.5194/acp-15-1769-2015, 2015.

Yan, C., Yin, R., Lu, Y., Dada, L., Yang, D., Fu, Y., Kontkanen, J., Deng, C., Garmash, O., Ruan, J., Baalbaki, R., Schervish, M., Cai, R., Bloss, M., Chan, T., Chen, T., Chen, Q., Chen, X., Chen, Y., Chu, B., Dällenbach, K., Foreback, B., He, X., Heikkinen, L., Jokinen, T., Junninen, H., Kangasluoma, J., Kokkonen, T., Kurppa, M., Lehtipalo, K., Li, H., Li, H., Li, X., Liu, Y., Ma, Q., Paasonen, P., Rantala, P., Pileci, R. E., Rusanen, A., Sarnela, N., Simonen, P., Wang, S., Wang, W., Wang, Y., Xue, M., Yang, G., Yao, L., Zhou, Y., Kujansuu, J., Petäjä, T., Nie, W., Ma, Y., Ge, M., He, H., Donahue, N. M., Worsnop, D. R., Veli-Matti Kerminen, Wang, L., Liu, Y., Zheng, J., Kulmala, M., Jiang, J., and Bianchi, F.: The Synergistic Role of Sulfuric Acid, Bases, and Oxidized Organics Governing New-Particle Formation in Beijing, Geophys. Res. Lett., 48, 1–12, https://doi.org/10.1029/2020GL091944, 2021.

Yang, L., Nie, W., Liu, Y., Xu, Z., Xiao, M., Qi, X., Li, Y., Wang, R., Zou, J., Paasonen, P., Yan, C., Xu, Z., Wang, J., Zhou, C., Yuan, J., Sun, J., Chi, X., Kerminen, V. M., Kulmala, M., and Ding, A.: Toward Building a Physical Proxy for Gas-Phase Sulfuric Acid Concentration Based on Its Budget Analysis in Polluted Yangtze River Delta, East China, Environ. Sci. Technol., 55, 6665–6676, https://doi.org/10.1021/acs.est.1c00738, 2021.

Yao, L., Garmash, O., Bianchi, F., Zheng, J., Yan, C., Paasonen, P., Sipilä, M., Wang, M., Wang, X., and Xiao, S.: Atmospheric new particle formation from sulfuric acid and amines in a Chinese megacity, Science (80-.)., 281, 278–281, 2018.

Yu, H., Ren, L., and Kanawade, V. P.: New Particle Formation and Growth Mechanisms in Highly Polluted Environments, Curr. Pollut. Reports, 3, 245–253, https://doi.org/10.1007/s40726-017-0067-3, 2017.

Yue, D., Hu, M., Wu, Z., Wang, Z., Guo, S., Wehner, B., Nowak, A., Achtert, P., Wiedensohler, A., Jung, J., Kim, Y. J., and Liu, S.: Characteristics of aerosol size distributions and new particle formation in the summer in Beijing, J. Geophys. Res. Atmos., 114, 1–13, https://doi.org/10.1029/2008JD010894, 2009.

Zhang, R., Khalizov, A., Wang, L., Hu, M., and Xu, W.: Nucleation and Growth of Nanoparticles in the Atmosphere, Chem. Rev., 112, 1957–2011, https://doi.org/10.1021/cr2001756, 2012.

Zhang, R., Wang, G., Guo, S., Zamora, M. L., Ying, Q., Lin, Y., Wang, W., Hu, M., and Wang, Y.: Formation of Urban Fine Particulate Matter, Chem. Rev., 115, 3803–3855, https://doi.org/10.1021/acs.chemrev.5b00067, 2015.

Zhang, Y., Tao, J., Ma, N., Kuang, Y., Wang, Z., Cheng, P., Xu, W., Yang, W., Zhang, S., Xiong, C., Dong, W., Xie, L., Sun, Y., Fu, P., Zhou, G., Cheng, Y., and Su, H.: Predicting cloud condensation nuclei number concentration based on conventional measurements of aerosol properties in the North China Plain, Sci. Total Environ., 719, 137473, https://doi.org/10.1016/j.scitotenv.2020.137473, 2020.

Zhou, Y., Dada, L., Liu, Y., Fu, Y., Kangasluoma, J., Chan, T., Yan, C., Chu, B., Daellenbach, K. R., Bianchi, F., Kokkonen, T. V., Liu, Y., Kujansuu, J., Kerminen, V. M., Petäjä, T., Wang, L., Jiang, J., and Kulmala, M.: Variation of size-segregated particle number concentrations in wintertime Beijing, Atmos. Chem. Phys., 20, 1201–1216, https://doi.org/10.5194/acp-20-1201-2020, 2020.